# On North Atlantic Interdecadal Variability: A Stochastic View

M. Latif, A. Timmermann, A. Grötzner,
C. Eckert, and R. Voss[1)]

Max-Planck-Institut für Meteorologie
Bundesstr. 55, D-20146 Hamburg, Germany

[1)] Deutsches Klimarechenzentrum
Bundesstr. 55, D-20146 Hamburg, Germany

## Abstract

We investigate in this paper the dynamics and predictability of North Atlantic interdecadal variability. Observations of the last hundred years reveal the existence of substantial interdecadal variability in both the ocean and the atmosphere in the North Atlantic region, and it is obvious that the interdecadal changes in both climate sub-components are linked to each other. One has therefore to consider the North Atlantic interdecadal variability within a coupled ocean-atmosphere framework.

The simplest paradigm for the generation of interdecadal variability is the stochastic climate model scenario. The ocean integrates the high-frequency weather noise (the variations arising from the passage of low and high pressure systems) giving rise to slow variations in the ocean's surface temperature, for example. The stochastic climate model concept explains one of the main characteristics of typical climate spectra, namely their redness. While the simplest version of the stochastic climate model yields relatively featureless spectra, spectral peaks also can be understood within the concept of the stochastic climate model, with the atmospheric noise exciting (damped) eigenoscillations of the ocean or the coupled ocean-atmosphere system.

The results of a multi-century integration with a coupled ocean-atmosphere general circulation model are largely consistent with the stochastic climate model. Two distinct modes exist in the North Atlantic region: A 15-year mode and a 35-year mode. Both modes depend critically on ocean-atmosphere interactions and must be regarded as inherently coupled air-sea modes. The memory of both modes, however, resides in the ocean. While the 15-year mode appears to be related to variations in the subtropical gyre circulation, the 35-year mode is related to variations in the thermohaline circulation. Predictability experiments with the coupled model indicate that subsurface quantities in the North Atlantic may be predictable one to two decades in advance, while surface quantities seem to be predictable only for a few years. These results imply that the coupling between the ocean and the atmosphere (although critical for the existence of interdecadal modes) is too weak to influence significantly the predictability characteristics of the atmosphere at decadal time scales.

## 1. Introduction

The North Atlantic climate system is characterized by considerable interdecadal variability. We show examples of interdecadal variability in Figs. 1 and 2. One of the main modes of the atmosphere over the North Atlantic is the North Atlantic Oscillation (NAO) (e. g. van Loon and Rogers (1978), Hurrell (1995)). The NAO is a dipole in sea level pressure (SLP), with centers of action near Island and the Azores (Fig. 1b), originally described by Walker (1924) and Walker and Bliss (1932). Hurrell (1995) defined an index of the NAO by the difference of the SLPs measured at Lisbon (Portugal) and Stykkisholmur (Iceland). Its time evolution (Fig. 1a) exhibits considerable interdecadal variability, with a maximum during the beginning of this century, a minimum during the 1960s, and strongly increasing values thereafter up to present. Moreover, there are observed fairly regular quasi-decadal [O(10 years)] variations during the most recent decades. The relatively strong upward trend observed during the last 20 years which contributed strongly to the rise in mean Northern Hemisphere surface temperature (Hurrell (1996)) has been the matter of intense scientific debate, since it is not clear as to whether this trend reflects greenhouse warming or is simply an expression of interdecadal variability.

Similar low-frequency variations on interdecadal time scales can be observed in the North Atlantic Ocean (Fig. 2). The potential temperature in the Labrador Sea in the depth range 800-2000m (curve labeled c), which is a good index of convection in this region, exhibits a time evolution, which is highly anti-correlated with the NAO index (Dickson et al. (1996)). Colder (warmer) temperatures imply stronger (weaker) convection, so that the cooling trend observed in the Labrador Sea since 1970 can be identified with enhanced convection. Interdecadal changes are also observed in the convective activity in the Greenland Sea (Fig. 2d) and in the salinity of the Sargasso Sea (Fig. 2e). The behaviours in the Labrador and Greenland Seas during the recent decades can be readily understood by atmospheric forcing. As the NAO strengthened and the Icelandic low intensified during the last few decades, more polar air masses are blown over the Labrador Sea, resulting in colder SSTs and stronger convection. Likewise temperatures in the Greenland Sea rised and convection weakened. This is visualized by Fig. 3 which shows the trends in SST and SLP observed over the last few decades. The trend in sea level pressure (Fig. 3b) is very similar to the NAO pattern (Fig. 1b), and consistent with a change in the NAO, the SSTs in the northern North Atlantic cooled, while they warmed further to the south (Fig. 3a). On the one hand, the surface temperature pattern can be explained as the response of the ocean to the surface heat flux changes that result from the change in the NAO. On the other hand, the SST anomaly pattern may well force a change in the NAO, as shown by Rodwell et al. (1999). Thus, one has to consider the interdecadal variability within the framework of large-scale air-sea interactions, as originally suggested by Bjerknes (1964).

We like to note one further interesting feature. As described above, the NAO exhibits quite strong quasi-decadal variations during the recent decades (Fig. 1a). These fluctuations are not seen in the convection indices of the Labrador and Greenland Seas (Figs. 2c and 2d), while decadal variations are obvious in the upper ocean salinity time series of the Sargasso Sea (Fig. 2e) and the subsurface temperature at ocean weather ship 'C' (52.5°N, 35.5°W) which is shown in Fig. 4. Furthermore, the quasi-decadal variations in the NAO and those shown in Figs. 2e and Fig. 4 are not coherent. This may point towards different mechanisms for the generation of the decadal variabilities.

Different mechanisms were put foreward to explain the interdecadal variability in general. On the one hand, external forcing mechanisms have been discussed for a long time. Variations in

the incoming solar radiation, for instance, were proposed as one of the major sources of interdecadal variability (e. g. Labitzke (1987), Lean et al. (1995)). Cubasch et al. (1997) show indeed that some climate impact of the sun might exist on time scales of many decades and longer by means of a coupled model experiment prescribing variations in the incoming solar radiation, but it is fairly controversial at present how strong the fluctuations in the solar insolation actually are. The forcing of interdecadal climate variability by volcanos is well established and therefore less controversial, and major volcanic eruptions can be easily seen in regional and globally averaged temperature records (e. g. Robock and Mao (1995)).

On the other hand, interdecadal variability arises from interactions within and between the different climate sub-systems. The two most important climate sub-systems are the ocean and the atmosphere. Non-linear interactions between different space and time scales can produce interdecadal variability in both the ocean (e. g. Jiang et al. (1996), Spall (1996)) and the atmosphere (e. g. Lorenz (1963), James and James (1989)) as shown by many modeling studies. More important in the generation of interdecadal variability, however, seem to be the interactions between the ocean and the atmosphere. The stochastic climate model scenario proposed by Hasselmann (1976) is a 'one-way' interaction: The atmospheric 'noise' (the random weather fluctuations) drives low-frequency changes in the ocean, leading to a red spectrum in the ocean's sea surface temperature (SST), for instance. It has been shown that the interannual variability in the midlatitudinal upper oceans is consistent with Hasselmann's (1976) stochastic climate model (e. g. Frankignoul and Hasselmann (1977)). This concept has been generalized recently by Frankignoul et al. (1997) who incorporated the wind-driven ocean gyres into the stochastic climate model concept, which extends the applicability of the stochastic climate model to interdecadal time scales. The atmospheric noise can excite also damped eigenmodes of the ocean circulation on interdecadal to centennial time scales, as shown, for instance, by the model studies of Mikolajewicz and Maier Reimer (1990), Weisse et al. (1994), and Griffies and Tziperman (1995).

'Two-way' interactions between the ocean and the atmosphere were also proposed to cause interdecadal climate variability (e. g. Latif and Barnett (1994), Gu and Philander (1997), Chang et al. (1997)). Similar to the El Niño/Southern Oscillation (ENSO) phenomenon (e. g. Philander (1990), Neelin et al. (1994)) ocean and atmosphere reinforce each other, so that perturbations can grow to climatological importance. The memory of the coupled system (which resides generally in the ocean) provides delayed negative feedbacks which enable continuous oscillations that are forced by the internal noise within the coupled ocean-atmosphere system. The relative roles of the noise and non-linearities in the context of interdecadal variability, however, needs to be addressed further.

We shall investigate in this paper the interdecadal variability in the North Atlantic region only. There are many other regions which exhibit strong interdecadal variability, such as the tropical and North Pacific regions. Latif and Barnett (1994), for instance, postulate the existence of an interdecadal cycle in the North Pacific, and Gu and Philander (1997) put forward the idea of a coupled tropical Pacific-North Pacific interdecadal cycle. It is beyond the scope of this paper to address all the different aspects of interdecadal variability. The reader is referred to the observational papers of e. g. Folland et al. (1986), Dickson et al. (1988), Mysak et al. (1990), Deser and Blackmon (1993), Kushnir (1994), Trenberth and Hurrell (1994), Mann and Park (1994), Levitus and Antonov (1995), Zhang et al. (1997), Mantua et al. (1997) and references therein for further information on the observational aspects of interdecadal variability. A fairly comprehensive overview of the different aspects of interdecadal variability (including theoretical, modeling, and observational aspects) can be found in the recent book published by Anderson and

Willebrand (1996), while an overview of the interdecadal variability simulated in coupled ocean-atmosphere models is given in the review article by Latif (1998).

The paper is organized as follows. We describe briefly the stochastic climate model concept and show some observational results supporting it in section 2. Section 3 deals with the quasi-decadal variability that arises from variations in the North Atlantic subtropical gyre circulation, as simulated by our coupled ocean-atmosphere model. We present the interdecadal variability associated with the North Atlantic thermohaline circulation of the same model in section 4. The predictability of interdecadal changes, as derived by classical predictability experiments, is addressed is chapter 5. The paper is concluded with a discussion in section 6.

## 2. The stochastic climate model

In contrast to the atmosphere, which has variations with typical time scales of a few days, the ocean is much more inert. Anomalies of the sea surface temperature (SST), for instance, persist typically for several months, while the characteristic time scale for the deep ocean is of the order of thousand years. Many aspects of the interactions between climate-subsystems with considerably different time scales can be described analogous to the Brownian motion in statistical physics. The picture is that oceanic anomalies (such as SST anomalies) result from the integration of many statistically independent atmospheric events, e. g. the passage of high and low pressure systems. One may view the SST variability, for instance, as the result of the integration of the surface heat flux anomalies within the oceanic mixed layer. This kind of interaction was introduced by Hasselmann (1976) and is referred to as the 'stochastic climate model'. The stochastic climate model scenario is a relatively simple concept which may be regarded as a kind of 'null hypothesis' for the generation of climate variability in general and decadal variability in particular.

The time evolution of a typical oceanic quantity y (such as SST) may be described by a Langevin equation

$$y'(t) = -\lambda y(t) + \xi(t), \quad (1)$$

with $\lambda$ representing a damping parameter and $\xi$ the atmospheric forcing that is assumed to be white noise. The oceanic response $G(\omega)$ is given within this concept by

$$G(\omega) = \sigma^2/(\lambda^2+\omega^2), \quad (2)$$

Here, $\omega$ denotes the frequency and $\sigma$ the standard deviation of the white noise forcing. We present in Fig. 5 schematically the spectra that result from the simplest version of the stochastic climate model (1). The atmospheric input spectrum (e. g. that of the surface heat flux) is assumed to be white noise, i. e. the spectral density does not depend on frequency. The oceanic response spectrum is red, with a slope $\omega^{-2}$ down to a frequency that depends on the damping $\lambda$. At frequencies smaller than $\lambda$ the oceanic spectrum is flat (white). It should be noted that no response of the atmosphere to the variations in the ocean is considered here. It is generally assumed, however, that such a feedback exists, at least at low frequencies, which would explain some of the interdecadal variability observed in the atmosphere (e. g. the NAO, see Fig. 1a).

Spectra computed from atmospheric and oceanic observations taken at ocean weather ship 'I'

(60.8°N, 20.6°W) support the stochastic climate model idea (e. g. Frankignoul and Hasselmann (1977), Hall and Manabe (1997)). This is visualized by Fig. 6 which shows spectra of anomalous SST and sea surface salinity (SSS) taken at weather ship 'I'. By and large the two spectra are consistent with the stochastic climate model, and a perfect red noise spectrum is not an unreasonable fit over the entire frequency range.

We expect according to the stochastic climate model that the spectrum of the SST anomalies flatens at a higher frequency relative to that of the SSS anomalies. The damping for SSS anomalies is considerably weaker than that for SST anomalies, which is due to the fact that the anomalous fresh water flux does not depend directly on the SSS anomalies, while the anomalous surface heat flux does usually depend critically on the SST and tends to damp its anomalies (a counter example, however, will be shown in section 3). A spectral analysis from the North Pacific (Hall and Manabe (1997)), for instance, confirms this. Since the decay time scales for SST and SSS anomalies in the North Atlantic are not different (Fig. 6) and the variations in SST and SSS coherent beyond frequencies of about 1/yr (Hall and Manabe (1997), not shown), one may conclude that non-local processes are also important in generating low-frequency variability in the North Atlantic. Such processes may be associated with changes in the large-scale ocean circulation and resultant changes in the advection of heat and salt, as described below.

In contrast to the spectra shown in Fig. 5 which result from the simplest version of the stochastic climate model, some spectra computed from observations in the North Atlantic region show also peaks (e. g. Deser and Blackmon (1993)). These peaks can be also explained by the stochastic climate model concept (e. g. Mikolajewicz and Maier-Reimer (1990)), and resonant interactions between the ocean and the atmosphere play a key role. The ocean or the coupled ocean-atmosphere system may support damped eigenoscillations that are excited by the noise (i. e. stochastic forcing) in the system (like a swing in the wind). A good prototype for such a scenario, according to which damped oscillations are excited by the stochastic forcing inherent to the system, is the stochstically forced harmonic oscillator

$$y''(t) + \lambda y'(t) + \omega_o^2 y(t) = \zeta(t) \quad (3)$$

Here $\omega_0$ is the eigenfrequency, and the meaning of the other symbols is as in (1). The oceanic response $G(\omega)$ is given by

$$G(\omega) = \sigma^2/[(\omega^2-\omega_o^2)^2 + \omega^2\lambda^2] \quad (4)$$

Such a generalized concept yields peaks at resonant frequencies $\omega_r$ which depend on the eigenfrequencies $\omega_0$ and the damping $\lambda$

$$\omega_r = (\omega_o^2 - \lambda^2/2)^{1/2} \quad (5)$$

The peaks will be generally superimposed on a red background spectrum which results from the 'pure' integration of the noise according to (1). In the case of an 'ocean-only' mode, in which the feedback from the ocean to the atmosphere is not important to the existence of the mode, the stochastic theory predicts a peak in the oceanic spectrum only, while a typical atmospheric spectrum is white (Fig. 7a). Such a situation corresponds to the mode described by Delworth et al. (1993) investigating the results of a coupled model simulation, as discussed in detail by Griffies and Tziperman (1995). In the case of the excitement of a 'coupled ocean-atmosphere' mode by the stochastic forcing, in which ocean and atmosphere are controlled by the boundary conditions of the respective other component, peaks will be found in both atmospheric and oceanic spectra,

as it is the case for the El Niño/Southern Oscillation phenomenon (e. g. Philander (1990)). This situation is shown schematically in Fig. 7b and may apply to the modes simulated by some coupled models in the North Atlantic, as described by Grötzner et al. (1998) and Timmermann et al. (1998). It is plausible to assume that those eigenmodes will be excited preferably which have surface expressions that match those of the stochastic forcing (this is usually referred to as 'spatially resonant interaction').

We would like to point out another class of stochastically forced variability. The internal atmospheric variability can be decomposed into relatively few spatial patterns such as the Pacific North America (PNA) pattern or the North Atlantic Oscillation. If oceanic advection is included in the stochastic climate model (1), peaks in oceanic spectra are possible, although the atmospheric forcing is still white in time. The spatial coherence of the atmospheric forcing in concert with the mean currents are able to produce distinct time scales, and a peak in ocean spectra may be found at the frequency $\omega = k_0 u$, with $k_0$ the dominant wavenumber of the atmospheric forcing and u the mean current velocity advecting oceanic anomalies. Such type of stochastically forced variability was proposed by Lemke et al. (1980), Frankignoul and Reynolds (1983), Sutton and Allen (1997), Saravanan and McWilliams (1997), and Weisse et al. (1997). The latter attribute the dynamics of the Antarctic Circumpolar Wave (ACW, White and Peterson (1996)) to such a stochastic climate model with advection, while Sutton and Allen (1997) and Saravanan and McWilliams (1997) explain part of the North Atlantic low-frequency variability by this mechanism.

In summary, the stochastic forcing of the climate system by the noise inherent to it is an important mechanism in generating climate variability. The shape of the spectra derived from observations (or model simulations) may provide important indications for the underlying dynamics leading to the variability considered. If the variability is consistent with the simple version (1) of the stochastic climate model, one may assume that ocean dynamics are not important, and that the variability arises from the integration of the atmospheric weather noise by the oceanic mixed layer. If (statistically significant) peaks are found, this points generally towards a prominent role of the ocean dynamics in producing the variability at decadal time scales. We shall show two such examples below which were both derived from a multi-century simulation with a coupled ocean-atmosphere general circulation model.

## 3. Quasi-decadal variability in the North Atlantic

We turn now to the integration with our coupled ocean-atmosphere general circulation model (ECHAM3/LSG). Details of the coupled model and the integration can be found in Voss et al. (1998), Timmermann (1996) and Timmermann et al. (1998). The coupled model was integrated for 2000 years, and the analyses shown below were performed using annually averaged values. The coupled model simulates reasonably well the low-frequency variability in the North Atlantic, which is shown by the comparison of the standard deviations of annually averaged SSTs as computed from observations and the coupled model simulation (Fig. 8).

One can separate conceptually the ocean circulation in the North Atlantic into a 'wind-driven' and a 'thermohaline' part. The former is forced by the surface wind stress and associated with horizontal circulations in the upper ocean (subtropical and subpolar gyres), while the latter is associated with a meridional (north-south) circulation and deep convection in the northern North Atlantic. We shall show that variations in both types of circulation systems can lead to

interdecadal variability. Since the adjustment times of the gyre circulations are considerably shorter than that of the thermohaline circulation, variations associated with the gyres have typical time scales of about 10-20 years (quasi-decadal), while those linked to the thermohaline circulation have typical time scales of several decades (interdecadal). Interestingly, both types of variability seem to co-exist in the coupled model simulation. as shown below, and there are some indications from observations that this is the case in the real world too (e. g. Deser and Blackmon (1993)).

We present in Figs. 9 and 10 time series and spectra of model-simulated anomalous North Atlantic SST, meridional overturning (an index of the strength of the thermohaline circulation) and SLP. It is obvious from the time series that low-frequency variations are much more pronounced in the ocean (Figs. 9a and 9c) than in the atmosphere (Fig. 9b). Consistent with the stochastic climate model picture, the spectra of the SST and overturning anomalies are red (Figs. 10a and 10b), while that of the anomalous SLP is (almost) white (Fig. 10c). At periods of about 15 and 35 years, however, both the SST and SLP spectra exhibit peaks, which indicates that two coupled modes may exist. The 35-year peak only is found in the spectrum of the anomalous overturning, which indicates that the interdecadal variability is connected to variations in the models's thermohaline circulation. The significance of the spectral peaks was assessed by testing the spectra against the null hypothesis, that the variability can be described by a first-order autoregressive process (which would result from the simplest version (1) of the stochastic climate model). The spectral peaks are marginally significant, and the overall structures of the spectra indicate that the decadal and interdecadal modes are strongly damped and excited by the stochastic forcing. However, as shown below, the physics of the quasi-decadal variability differ strongly from those of the interdecadal variability (section 4). Thus, it makes sense to distinguish these two types of low-frequency variability from a physical point of view.

Our hypothesis for the generation of the quasi-decadal mode is that it arises from air-sea interactions and is associated with variations in the subtropical gyre circulation. In order to describe the spatial structure of the mode, we performed a Canonical Correlation Analysis (CCA) of the North Atlantic SST and SLP anomaly fields. The leading CCA mode (canonical correlation = 0.83) is connected to the quasi-decadal mode, which was inferred from the two CCA time series (not shown) which exhibit spectral peaks at a period of 15 years. The leading CCA mode explains 18% and 52% in the SST and SLP anomaly fields, respectively. The resulting SLP anomaly pattern (Fig. 11b) is the North Atlantic Oscillation (NAO), with opposite changes equatorward and poleward of about 50°N. The corresponding SST anomaly pattern (Fig. 11a) is a tripole with a band of positive anomalies in the region 20°N-40°N and negative anomalies to the north and south. These patterns are consistent with those shown by Deser and Blackmon (1993) and Grötzner et al. (1998), who derived the spatial SST and SLP structures of the quasi-decadal variability over the North Atlantic from observations.

The memory of the quasi-decadal mode resides in the ocean. This can be demonstrated by a POP-analysis of upper ocean heat content anomalies (see Timmermann (1996) for details). The leading POP mode explaining 21% of the variance has a decadal rotation period, as was revealed by a spectral analysis of the corresponding POP time series (Fig. 12). The evolution of the anomalous upper ocean heat content is dominated by a clockwise rotation around the subtropical gyre (Fig. 13). Advection of temperature anomalies by the mean currents and wave processes (in response to changing winds) are likely to contribute both to the evolution in the upper ocean heat content, as argued by Grötzner et al. (1998) studying the quasi-decadal variability in another coupled model. Thus, the time scale of the oscillation is probably set by a combination of advective and wave time scales, since both time scales are of the same order. The

importance of advection in the quasi-decadal variability was also highlighted by Sutton and Allen (1997) who investigated North Atlantic SST observations for the period 1945-1989.

In summary, the quasi-decadal variability in the North Atlantic region may be regarded as an eigenmode of the coupled ocean-atmosphere system, so that the interactions of the ocean and the atmosphere are crucial to the existence of the quasi-decadal mode. Ocean dynamics appear to be crucial in producing the oscillatory behaviour at the quasi-decadal time scale. We would like to point out, however, that the quasi-decadal mode is strongly damped (as it is in the observations) and that the bulk of the quasi-decadal variability may well be explained by the stochastic climate model scenario.

## 4. Interdecadal variability in the North Atlantic

On longer time scales, we expect that variations in the thermohaline circulation become more and more important. The adjustment time of the wind-driven gyres is of the order of one to two decades only (depending on the ocean basin considered), while the adjustment time of the thermohaline circulation ranges from decades to many centuries (depending on which portion of the global thermohaline circulation is considered). As can be inferred from Fig. 10, enhanced variability in both the ocean and the atmosphere is simulated at a period of about 35 years. We shall refer this type of interdecadal variability to as the 'interdecadal mode'. Since enhanced variability is simulated in both media at the 35-year time scale, our working hypothesis is (as for the quasi-decadal variability) that the variability arises from ocean-atmosphere interactions (see Timmermann (1996) and Timmermann et al. (1998) for further details).

The 35-year period is seen nicely in the spectrum of the overturning index (Fig. 10b). We used therefore the index of the meridional overturning (Fig. 9c) to describe the evolution of the interdecadal mode by computing lagged regression patterns of selected quantities (SLP, SST, fresh water flux, SSS, surface currents, and convection). In order to highlight the interdecadal variability, we band-pass filtered the model data prior to the regression analyses retaining variability with time scales of 25-45 years. The anomalous SST pattern ten years prior to the maximum overturning (lag -10 years) is characterized by negative anomalies which cover the entire North Atlantic Ocean, with maximum cold anomalies near 40°N (Fig. 14b). The associated SLP anomaly pattern is the North Atlantic Oscillation (NAO) in its reverse polarity (Fig. 14a). Important to the subsequent phase reversal are the positive salinity anomalies which develop primarily east of Newfoundland (Fig. 14d). As shown in Timmermann et al. (1998), this positive SSS anomaly is created by anomalous fresh water input (primarily through enhanced evaporation, Fig. 14c) and anomalous salt transport by anomalous Ekman currents (Fig. 14e). The convection at this time is near normal (Fig. 14f). The SSS anomaly has grown and expanded in area five years later (lag -5 years), as shown in Fig. 15d. At this time, the SLP and SST anomaly patterns are not well developed and in a kind of 'transition stage' (Figs. 15a and 15b). The convection, however, shows a clear intensification in the sinking region south of Greenland (Fig. 15f), in response to the enhanced density which is due to the increased sea surface salinity in this region. This will lead to a strengthened thermohaline circulation and subsequently to an enhanced poleward heat transport, which will in turn reverse the SST tendendy. This is visualized in Fig. 16b which shows positive SST anomalies that cover most of the North Atlantic at the time of the maximum overturning (lag 0). The SLP anomaly pattern has also reversed, with an intensified Icelandic low and Azorian high (Fig. 16a). The signals in the anomalous salinity and convection are now relatively weak (Figs. 16d and 16f). The anomalous SLP and SST pattern will

grow further, until half a cycle is completed at lag +5 years (not shown). A negative SSS anomaly develops through air-sea interactions at lag +5 years which will eventually reduce the density in the sinking region and weaken the convection. This will lead to a weakend thermohaline circulation, reduced poleward heat transport and a change towards anomalous cold temperatures in the North Atlantic, which completes a full cycle (not shown).

Thus, as for the quasi-decadal variability, large-scale air-sea interactions are important in generating the interdecadal variability. The atmospheric response to mid-latitudinal SST anomalies seems to be a key process for the generation of mid-latitudinal low-frequency variability on the time scales of decades. While the anomalous surface stress is important to the generation of the quasi-decadal variability, the anomalous fresh water flux is important to the generation of the interdecadal variability. In both types of variability, however, the air-sea coupling appears to be rather weak, and the resulting modes are rather strongly damped, as can be inferred from the spectral analyses presented above.

## 5. Predictability of interdecadal variability in the North Atlantic

After having discussed some aspects of the dynamics of the decadal and interdecadal variabilities in the North Atlantic, we would like to address now the question of the predictability at decadal time scales. We can distinguish three basic cases from the above discussion (Fig. 17). We consider first the 'pure' stochastic climate model. In this case, the predictability limit of oceanic quantities is given by their persistence (autocorrelation), which ranges typically from a few months (for surface quantities) to many years (for subsurface quantities). The predictability of the atmosphere at time scales beyond the predictability limit of individual weather phenomena, which is of the order of about fourteen days, is not affected, since no feedback from the ocean to the atmosphere is considered (Fig. 17a). The second case is the stochastically forced 'ocean-only' mode. Enhanced predictability relative to persistence is found for oceanic quantities around the resonance frequency, while atmospheric quantities cannot be predicted with higher skill relative to the 'pure' stochastic climate model (Fig. 17b). Thus, if an oceanic mode exists with a decadal period, the variations in the ocean associated with this mode will be predictable at decadal time scales. Finally, third, we consider the stochastically forced coupled ocean-atmosphere mode. Both atmospheric and oceanic quantities exhibit enhanced predictability (again relative to persistence) at the resonance frequency (Fig. 17c). An example of this latter case is the ENSO phenomenon, for which both oceanic (e. g. eastern equatorial SST anomalies) and atmospheric quantities (e. g. the Southern Oscillation Index) are predictable at lead times of about one year (for a recent review on ENSO predictability see e. g. Latif et al. (1998)). If coupled modes with decadal periods exist in the North Atlantic, both the atmosphere and the ocean will exhibit enhanced predictability at decadal time scales in the North Atlantic region. We have described two such modes from our coupled model simulation, and it will depend critically on the degree of damping, whether the coupled nature of the mode will affect significantly the predictability of the atmosphere at decadal time scales.

Thus, the predictability characteristics of the low-frequency variability in the North Atlantic can provide important informations about its underlying dynamics. We conducted therefore an ensemble of predictability experiments with our coupled model. Before we describe the results of the predictability experiments, we discuss briefly the spectral characteristics of the three key quantities (SST, overturning, NAO) shown in Fig. 10. All three spectra show peaks at a period

of 35 years. Most striking, however, is the difference in the amount of the high-frequency variability. While the overturning index exhibits relatively weak variability up to time scales of about one decade, the SST and NAO are characterized by much more high-frequency variability. Thus, the deep ocean acts as a kind of low-pass filter, and we expect that subsurface quantaties exhibit much more predictability at decadal time scales than surface or atmospheric quantities. In particular, it is likely that the interdecadal mode will be predictable in the subsurface ocean only, although all three quantities shown exhibit peaks at the period of 35 years. The amount of high-frequency noise in the SST and NAO is simply too high and destroys the predictability at relatively long time scales. Another factor limiting the predictability of the two modes discussed here is the width of the spectral peaks, implying a relatively strong damping of the modes.

We have applied our coupled ocean-atmosphere circulation model (which was also used to study the dynamics of the quasi-decadal and interdecadal variabilities; see sections 3 and 4) to assess systematically the predictability of climate variations in the North Atlantic region at decadal time scales (further details can be found in Grötzner et al. (1999)). Classical predictability experiments were conducted in ensemble mode. We have chosen four states from the control integration, from which the coupled model was restarted. While the oceanic initial conditions remained unchanged, the atmospheric conditions were perturbed. Each predictability ensemble comprises of ten individual members, i. e. for each of the four oceanic states ten experiments were performed with different atmospheric initial conditions. Each predictability experiment has a duration of twenty years (the duration in the last forecast ensemble amounts to only ten years). The divergence of the trajectories within an ensemble provides an indication of the predictability at decadal time scales. Our experimental setup yields an upper limit of decadal predictability, since we assume a perfect knowledge of the oceanic initial conditions, an assumption which will be never fulfilled in a real forecast situation.

We present in Figs. 18, 19, and 20 the results from our forecast ensembles. We present the results in terms of the leading EOFs of the anomalous meridional overturning, SST, and 500 hPa heigts. The individual forecast trajectories show relatively little spread , when the meridional overturning is considered (Fig. 18), which is visualized by the ensemble means and normalized ensemble variances. The variance was normalized using the variance computed from the control integration. When the normalized variance reaches unity, the variations between the individual forecast members are as large as typical variations in the control run, which defines a predictability limit. The North Atlantic meridional overturning is predictable for about one to two decades, depending on the forecast ensemble considered. The anomalous North Atlantic SST, however, appears not to be predictable beyond time lags of a few years (Fig. 19), which is also true for the leading EOF of the anomalous Northern Hemisphere 500 hPa heights (Fig. 20). This latter result, however, depends somewhat on the forecast ensemble considered: When predictability experiments are started from states characterized by strong SST anomalies, the predictability of anomalous SST and 500 hPa heights seems to be enhanced.

We anticipated these results from the spectral analyses shown in Fig. 10. Thus, our predictability experiments highlight the ocean's role in generating the interdecadal variability. Although the coupling between the ocean and the atmosphere seems also to play a key role in the generation of the quasi-decadal and interdecadal modes, the coupling appears to be too weak (or equivalently the damping too strong) to influence the predictability of surface quantities at decadal time scales in the presence of the internal high-frequency noise. The results of our predictability experiments are consistent with those shown by Griffies and Bryan (1997), who were the first to apply a coupled ocean-atmosphere model to investigate the decadal predictability in the

North Atlantic region.

## 6. Discussion

We have shown that the North Atlantic climate variability at decadal time scales is largely consistent with the picture that the noise immanent to the coupled ocean-atmosphere system drives its low-frequency variability. This stochastic concept is supported by observations, simulations and predictability experiments with a sophisticated coupled ocean-atmosphere general circulation model. Large-scale ocean-atmosphere interactions play an important role in the generation of the interdecadal variability, and eigenmodes of the coupled ocean-atmosphere may exist in the North Atlantic region. It is likely, however, that these eigenmodes are strongly damped.

In this article the stochastic climate model scenario served as a paradigm for the description of climate variations. Many observations and modeling results agree with its predictions. There are, however, alternative paradigms which as well capture essential features of climate variability. Imagine, for example, the NAO. One may hypothesize that the dynamics of this climate fluctuation may be represented by a low-dimensional non-linear system. Its attractor in phase space may consist of regions where the system stays for a relatively long time. These are the minima and maxima of the observed time series. Transitions between states occur quasi-regularly (see Lorenz (1963), Palmer (1993), and references therein for further details). The observational records do not permit a distinction between these two paradigms, since they are too short. In the near future long simulations with coupled ocean atmosphere GCMs could allow such inferences.

Our studies raise some important scientific questions that need to be addressed in more detail in the future. One of the most important challenges is to understand the atmospheric response to mid-latitudinal SST anomalies. This response is likely to be highly non-linear, since it involves changes in the statistics of the transient eddies (e. g. Palmer and Sun (1985)) which feed back onto the mean flow. We have reasons to believe that the atmosphere is indeed sensitive to mid-latitudinal SST anomalies, as argued by Latif and Barnett (1994). The spectral peaks in the model's NAO, the pan-oceanic connections between the North Atlantic and the North Pacific described by Timmermann et al. (1998), and additional atmospheric response experiments with prescribed SST anomalies (not shown), all of these indicate that the atmosphere feels the slowly changing North Atlantic SSTs. However, the internal atmospheric variability is relatively strong, and it remains unclear as to whether the atmosphere is affected by the slowly varying boundary conditions to a degree that enables useful predictions at decadal time scales.

The oceanic processes that lead to the interdecadal variations in the North Atlantic SST need also to be analysed in more detail. We need to quantify the relative contributions of mixed layer processes and ocean dynamics to the SST changes. This can be achieved, for instance, by conducting an experiment, in which the atmosphere is coupled to a fixed-depth mixed layer (slab) model. Such an experiment is underway, and its outcome will be discussed in a forthcoming paper. A series of experiments was performed by Manabe et al. (1996), who compare three thousand-year integrations: A fully coupled run with an ocean-atmosphere general circulation model, an atmosphere-slab run, and an atmosphere-only run with fixed climatogical SSTs. Our results presented in this paper are mostly consistent with the results of Manabe et al. (1996). In particular, Manabe et al. (1996) conclude that the stochastic forcing plays a major role in gen-

erating low-frequency variability.

Moreover, it would be desirable to understand the relative roles of changes in the wind-driven and thermohaline circulations in changing the North Atlantic SST. Sensitivity experiments with our coupled ocean-atmosphere model would help to get further insight into this matter. One could, for instance, inhibit certain atmospheric feedbacks in coupled integrations, such as the fresh water feedback or the wind stress feedback and compare the level of SST variability with that in the control run. Such experiments will provide important informations about the mechanisms that lead to the decadal and interdecadal variations in the SST. These experiments are underway, and we shall report on the their outcomes in forthcoming papers.

Finally, model verification is still an important issue. We have used so far relatively coarse-resolution models to investigate the dynamics and predictability of decadal and interdecadal variability. Such models have considerable problems in simulating important aspects of the global climate and its variability. Relatively large flux corrections, are applied to inhibit the coupled models to drift into unrealistic climates. It is unknown how these corrections affect the variability of complex non-linear systems such as the climate system. Furthermore, we have no good estimate of the space-time structure of the low-frequency variability from observations. Paleoclimatic datasets will become more and more important to validate the coupled models. An example of such a dataset, for instance, is the multi-century reconstruction of the North Atlantic Oscillation from tree rings (Cook et al. (1997)).

## Acknowlegements

The authors would like to thank Drs. G. Lohmann, E. Maier-Reimer, and U. Mikolajewicz for many fruitful discussions. This work was supported by the German government by its "Decadal Predictability" and "Ocean-CLIVAR" programmes and the European Union through its "DICE" and "SINTEX" projects. The model runs were conducted at the Deutsches Klimarechenzentrum in Hamburg.

## References

Anderson, D. L. T. and J. Willebrand, 1996: Decadal climate variability: Dynamics and Predictability. NATO ASI Series, Series I: Global Environmental Change, Vol. 44, Springer, 493 pp.

Bjerknes, J., 1964: Atlantic air-sea interaction. Adv. in Geophys., Academic Press, 10, pp 1-82.

Chang, P., L. Ji, and H. Li, 1997: A decadal climate variation in the tropical Atlantic Ocean from thermodynamic air-sea interactions. Nature, 385, 516-518.

Cook, E. R., R. D. D'Arrigo, and K. R. Briffa, 1997: A reconstruction of the North Atlantic Oscillation using tree-ring chronologies from North America and Europe. The Holocene, in press.

Cubasch U., R. Voss, G. Hegerl, J. Waszkewitz, T.J. Crowley, 1997: Simulation of the influence of solar radiation variations on the global climate with an ocean-atmosphere general circulation model. Clim. Dyn., 13, 757-767

Delworth, T., S. Manabe, and R. J. Stouffer, 1993: Interdecadal variations of the thermohaline circulation in a coupled ocean-atmosphere model. J. Climate, 6, 1993-2011.

Deser, C. and M. L. Blackmon, 1993: Surface climate variations over the North Atlantic ocean during winter: 1900-1989. J. Climate, 6, 1743-1753.

Dickson, R. R., J. Meincke, S.-A. Malmberg, A. J. Lee, 1988: The "Great Salinity Anomaly" in the northern North Atlantic 1968-1982. Prog. Oceanogr., 20, 103-151.

Dickson, R., J. Lazier, J. Meincke, P. Rhines, and J. Swift,1996: Long-term coordinated changes in the convective activity of the North Atlantic. Prog. Oceanogr., 38, 241-295.

Folland, C. K., T. N. Palmer, and D. E. Parker, 1986: Sahel rainfall and worldwide sea temperatures. Nature, 320, 602-607.

Frankignoul, C. and K. Hasselmann, 1977: Stochastic climate models. Part II: Application to sea surface temperature variability and thermocline variability. Tellus, 29, 284-305.

Frankignoul, C. and R. W. Reynolds, 1983: Testing a dynamical model for mid-latitude sea surface temperature anomalies. J. Phys. Oceanogr., 13, 1131-1145.

Frankignoul, C., P. Müller, and E. Zorita, 1997: A simple model of the decadal response of the ocean to stochastic wind forcing. J. Phys. Oceanogr., 27, 1533-1546.

Griffies, S. M. and E. Tziperman, 1995: A linear thermohaline oscillator driven by stochastic atmospheric forcing. J. Climate, 2440-2453.

Griffies, S. M. and K. Bryan, 1997: Ensemble predictability of simulated North Atlantic interdecadal climate variability. Science, 275, 181-184.

Grötzner, A., M. Latif, and T. P. Barnett, 1998: A decadal climate cycle in the North Atlantic Ocean as simulated by the ECHO coupled GCM. J. Climate, 11, 831-847.

Grötzner, A., M. Latif, A. Timmermann, and R. Voss, 1999: Interannual to decadal predictability in a coupled ocean-atmosphere general circulation model. J. Climate, in press.

Gu, D. and S.G.H. Philander, 1997: Interdecadal climate fluctuations that depend on excahnges between the tropics and extratropics. Science, 275, 805-807.

Hall, A., and S. Manabe, 1997: Can local linear stochastic theory explain sea surface temperature and salinity variability? Climate Dynamics, 13, 167-180.

Hasselmann, K., 1976: Stochastic climate models. Part I: Theory. Tellus, 28, 473-485.

Hurrell, J. W.,1995: Decadal trends in the North Atlantic Oscillation regional temperatures and precipitation. Science, 269, 676-679.

Hurrell, J. W, 1996: Influence of variations in extratropical wintertime teleconnections on Northern Hemisphere temperature. Geophys. Res. Lett., 23, 665-668.

James, I. N. and P. M. James, 1989: Ultra-low-frequency variability in a simple atmospheric model. Nature, 342, 53-55.

Jiang, S., F.-F. Jin, and M. Ghil. 1996 : Multiple equilibria, periodic, and aperiodic solutions in a wind-driven, double gyre, shallow-water model. J. Phys. Oceanogr., 25, 764-786.

Kushnir, Y., 1994: Interdecadal variations in the North Atlantic sea surface temperature and associated atmospheric conditions. J. Climate, 7, 141-157.

Labitzke, K., 1987: Sunspots, the QBO, and the stratospheric temperature in the north polar region. Geophys. Res. Lett., 14, 535-537.

Latif, M., 1998: Dynamics of interdecadal variability in coupled ocean-atmosphere models. J. Climate, 11, 602-624.

Latif, M. and T.P. Barnett, 1994: Causes of decadal climate variability over the North Pacific and North America. Science, 266, 634-637.

Latif, M., D. Anderson, T. Barnett, M. Cane, R. Kleeman, A. Leetmaa, J. O'Brien, A. Rosati, and E. Schneider, 1998: A review of the predictability and prediction of ENSO. J. Geophys. Res. (Oceans), 103, 14,375-393.

Lean, J., J. Beer, and R. Bradley, 1995: Reconstruction of solar irradiance since 1600: Implications for climate change. Geophys. Res. Lett., 22, 3195-3198.

Lemke, P., E. W. Trinkl, and K. Hasselmann, 1980: Stochastic dynamic analysis of polar sea ice variability. J. Phys. Oceanogr., 10, 2100-2120.

Levitus, S., T. P. Boyer, and J. Antonov, 1994: World Ocean Atlas1994. Volume 5: Interannual

variability of upper ocean thermal structure structure. U.S. Department of Commerce, NOAA, Washington, D. C.

Levitus S. and J. Antonov, 1995: Observational evidence of interannual to decadal-scale variability of the subsurface temperature-salinity structure of the world ocean. Climate Change, 31, 495-514, Kluwer Academic Publishers, The Netherlands.

Lorenz, E. N.,1963: Deterministic nonperiodic flow. J. Atmos. Sci., 20, 130-141.

Manabe, S. and R. J. Stouffer, 1996: Low-frequency variability of surface air-temperature in a 1000-year integration of a coupled atmosphere-ocean-land surface model. J. Climate, 9, 376-393.

Mann, M. E. and J. Park, 1994: Global-scale modes of surface temperature variability on interannual to century timescales. J. Geophys. Res., 9, 25819-25833.

Mantua, N. J., S. R. Hare, Y. Zhang, J. M. Wallace, and R.C. Francis, 1997: A Pacific interdecadal climate oscillation with impacts on salmon production. Bull. Amer. Meteorol. Soc., 78, 1067-1079.

Mikolajewicz, U. and E. Maier-Reimer, 1990: Internal secular variability in an ocean general circulation model. Climate Dynamics, 4, 145-156.

Mysak, L. A., D. K. Manak, and R. F. Mardsen, 1990: Sea-ice anomalies in the Greenland and Labrador Seas 1900-84 and their relation to an interdecadal Artctic climate cycle. Climate Dynamics, 5, 111-133.

Neelin, J. D., M. Latif, and F.-F. Jin, 1994: Dynamics of coupled ocean-atmosphere models: The tropical problem. Ann. Rev. Fluid Mech., 26, 617-659.

Palmer, T. N.,1993: A nonlinear dynamical perspective on climate change. Weather, 48, 313-348.

Palmer, T. N. and Z. Sun, 1985: A modelling and observational study of the relationship between sea surface temperature in the northwest Atlantic and the atmospheric general circulation. Quart. J.R. Meteorol. Soc., 111, 947-975.

Philander, S. G. H., 1990: El Niño , La Niña, and the Southern Oscillation. Academic Press, Inc., San Diego, 293 pp.

Robock, A. D. and J. Mao, 1995: The volcanic signal in surface temperature observations. J. Climate, 8, 1086-1103.

Rodwell, M. J., D. P. Rowell, and C. K. Folland, 1999: Oceanic forcing of the wintertime North Atalntic Oscillation and European climate. Nature, 398, 320-323.

Saravanan, R. and J. C. McWilliams, 1997: Stochasticity and spatial resonance in interdecadal climate fluctuations. J. Climate, 10, 2299-2320.

Spall, M. A., 1996: Dynamics of the Gulf Stream/Deep western boundary current crossover.

Part II: Low-frequency internal oscillations. J. Phys. Oceanogr., 26, 2169-2182.

Sutton, R. T. and M. R. Allen, 1997: Decadal predictability in Gulf Stream sea surface temperatures. Nature, 388, 563-567.

Timmermann, A., 1996: Modes of variability as simulated by a global climate model. PhD thesis. Available from Max-Planck-Institut für Meteorologie, Bundesstr.55, D-20146 Hamburg, Germany.

Timmermann, A., M. Latif, R. Voss, and A. Grötzner, 1998: North Atlantic interdecadal variability: A coupled air-sea mode. J. Climate, 11, 1906-1931.

Trenberth, K. E. and J. W. Hurrell, 1994: Decadal atmosphere-ocean variations in the Pacific. Climate Dynamics, 9, 303-319.

van Loon, H. and J. C. Rogers, 1978: The seasaw in winter temperatures between Greenland and Northern Europe. Part I: General description. Mon. Wea. Rev., 106, 296-310.

Voss, R., R. Sausen, and U. Cubasch,1998: Periodically synchronously coupled integrations with the atmosphere-ocan general circulation model ECHAM3/LSG. Climate Dynamics, 14, 249-266..

Walker, G. T., 1924: Correlations in seasonal variations of weather, IX. Mem. Indian. Meteor. Dept., 24, 275-332.

Walker, G. T. and E. W. Bliss, 1932: World Weather V. Mem. Roy. Meteor. Soc., 4, 53-84.

Weisse, R., U. Mikolajewicz, and E. Maier-Reimer, 1994: Decadal variability of the North Atlantic in an ocean general circulation model. J. Geophys. Res. (Oceans), 99, 12411-12421.

Weisse, R., U. Mikolajewicz, A. Sterl, and S. S. Drijfhout, 1997: Stochastically forced variability in the Antarctic Circumpolar Current. J. Geophys. Res. (Oceans), 104, 11,049-064.

White, W. B and R. G. Peterson, 1996: An Antarctic Circumpolar Wave in surface pressure, wind, temperature, and se-ice extent. Nature, 380, 699-702.

Zhang, Y., J. M. Wallace, and D. S. Battisti, 1997: ENSO-like interdecadal variability: 1900-93. J. Climate, 10, 1004-1020.

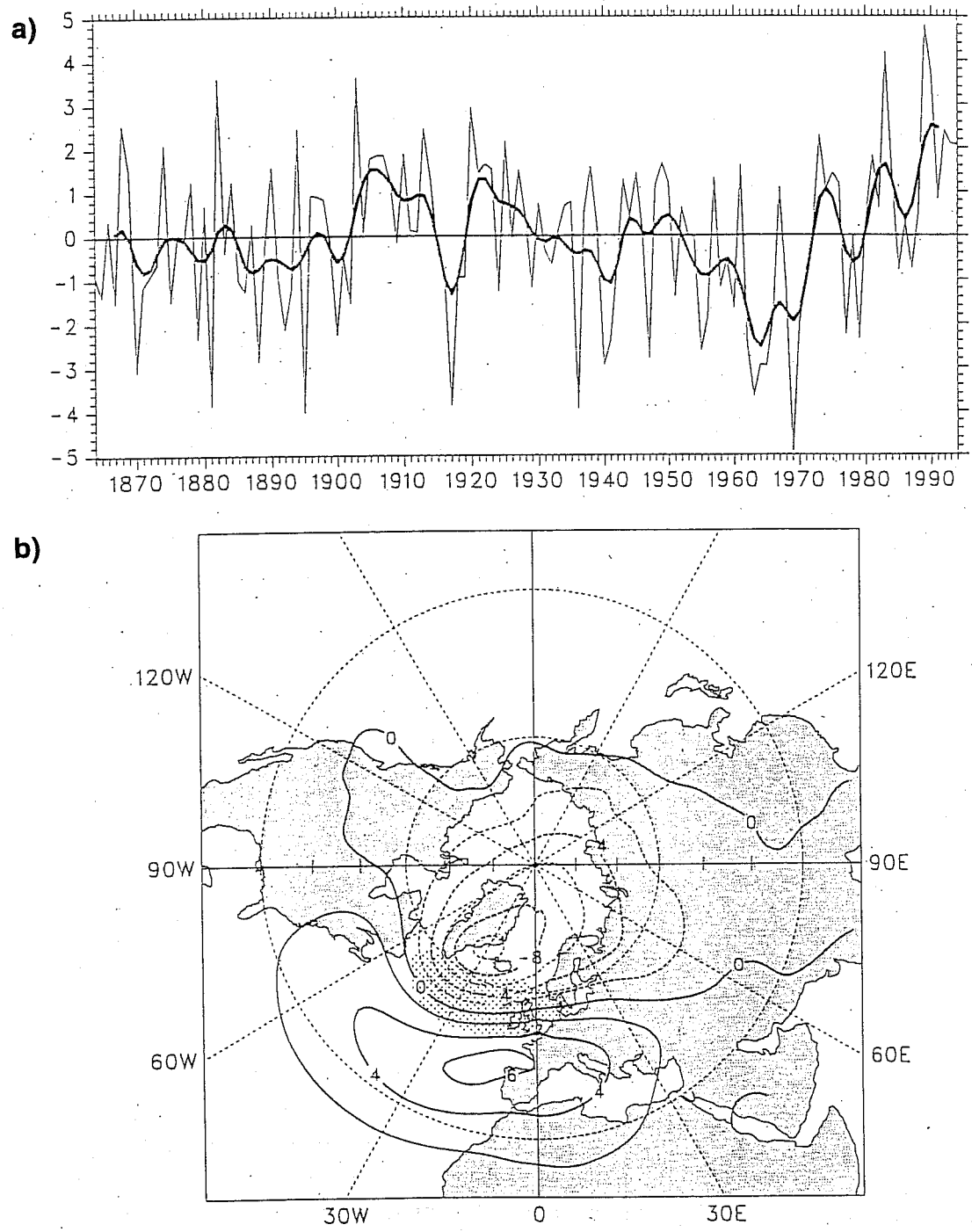


Fig.1: a) Time series of the North Atlantic Oscillation (NAO) index as defined by the normalized SLP difference between Lisbon (Portugal) and Stykkisholmur (Iceland). b) Spatial pattern of the NAO as defined by the difference in SLP between 'high' and 'low NAO index' winters. From Hurrell (1995).

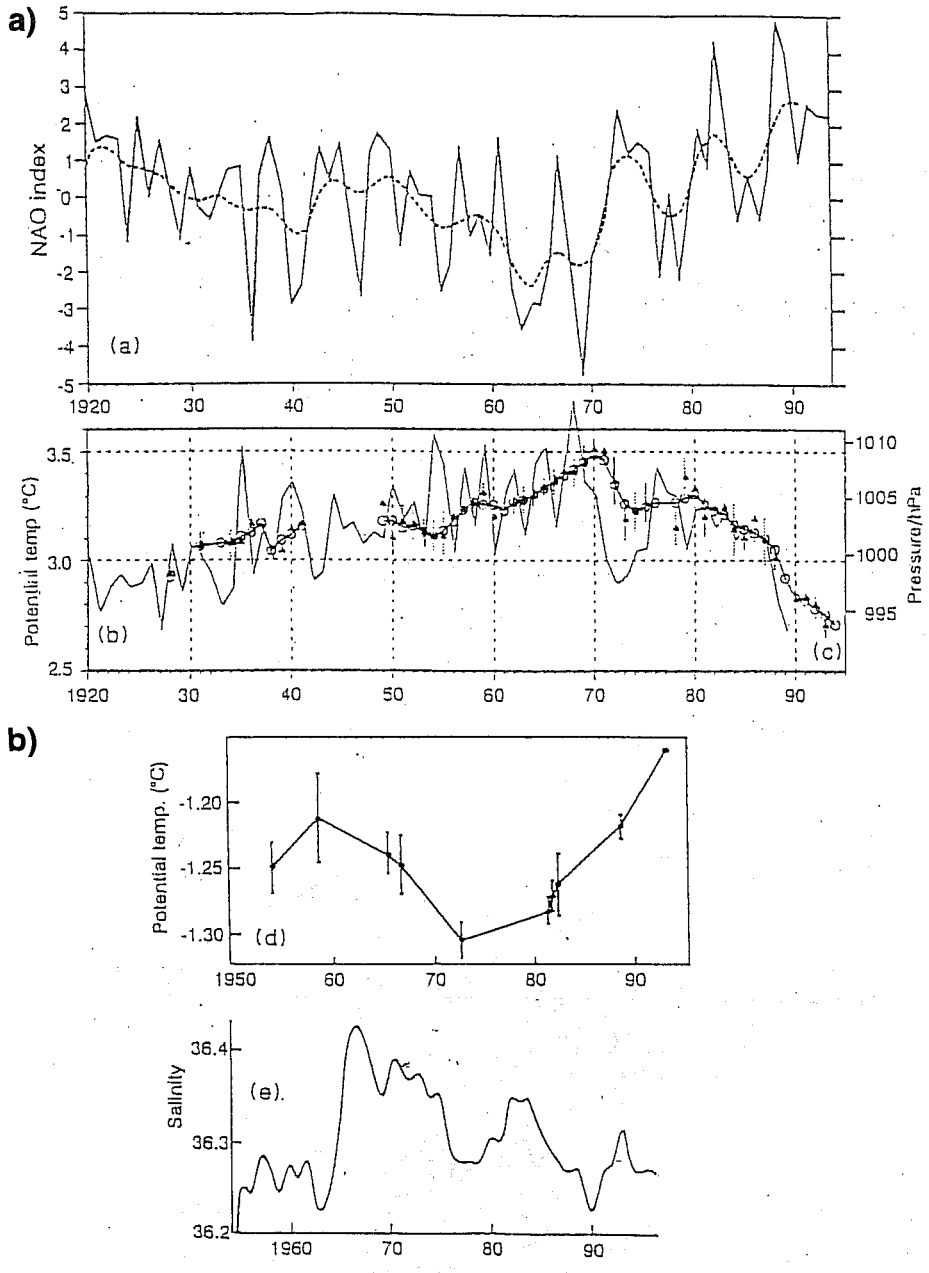


Fig. 2: Time series which vizualize the connection of atmospheric and oceanic changes at decadal time scales. a) NAO index (DJFM), b) mean SLP for western Greenland (DJF), c) potential temperature within the layer of minimum potential vorticity in the Labrador Sea, d) mean potential temperature in the Greenland Sea below 2000m, e) salinity on the density surface $\sigma_\theta$=26.6 off Bermuda. From Dickson et al. (1996).

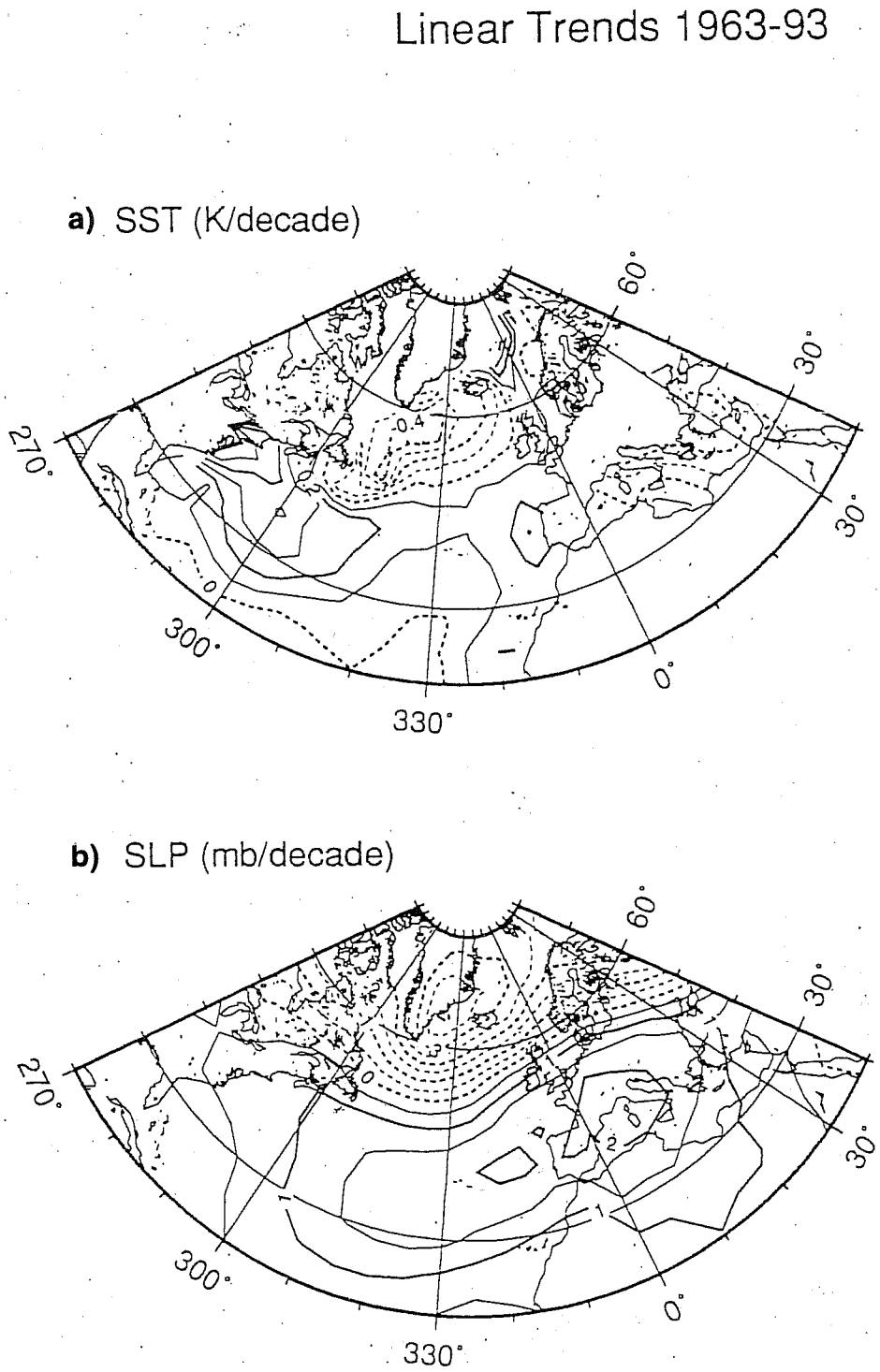


Fig. 3: Observed linear trends calculated for winter (DJF) December 1963 - February 1993 in a) SST (°C/decade), and b) SLP (hPa/decade). From Robertson (1998, pers. comm.)

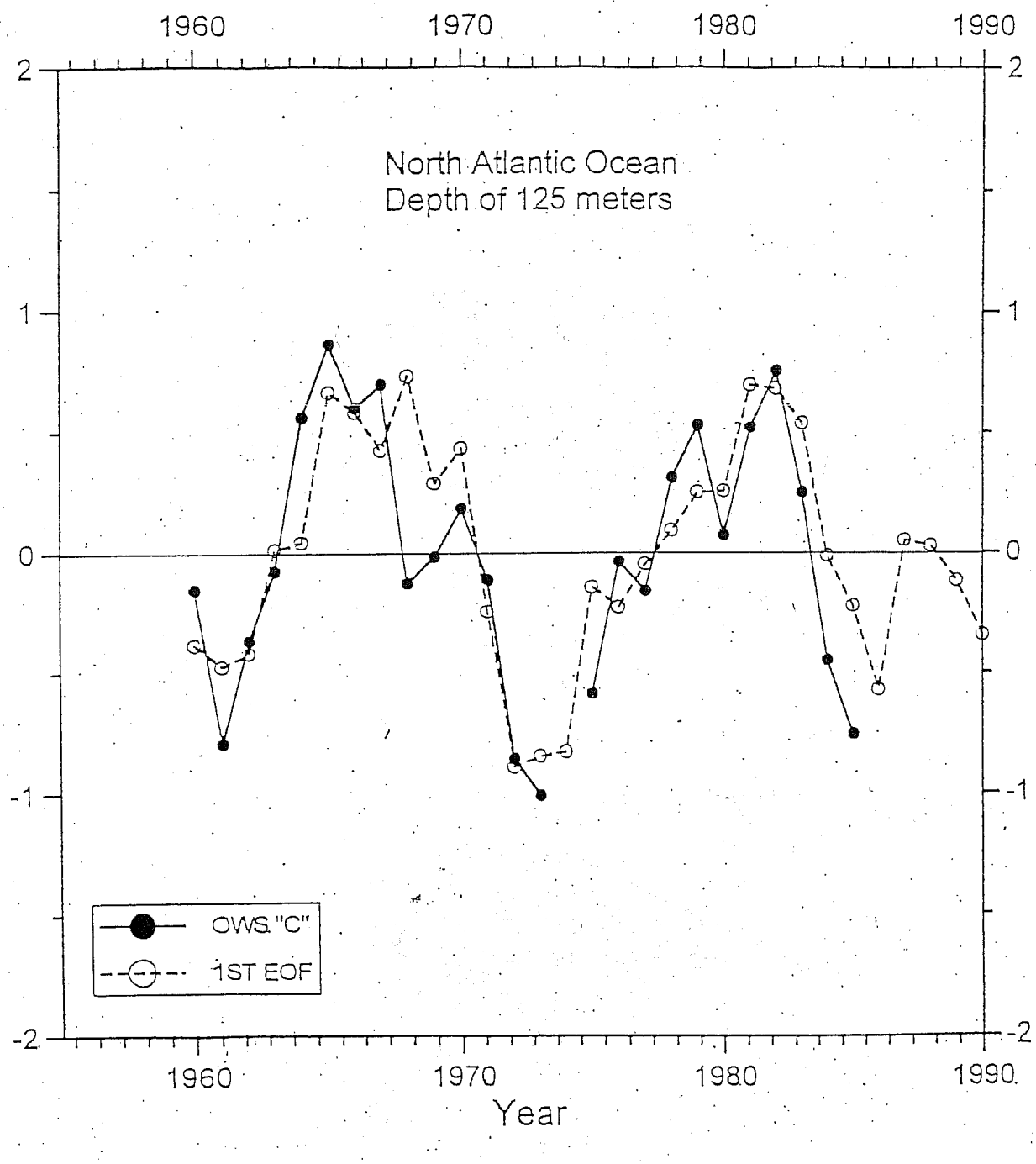


Time series of 1ST EOF (multiplied by -1) of North Atlantic temperature anomalies and temperature residuals about linear trend for 1960-85 at OWS "C" at 125 m depth

Fig.4: Time series of the first EOF (multiplied by -1) of North Atlantic temperature anomalies and temperature residuals about linear trend for 1960-1985 at ocean weather ship 'C' (52.5°N, 35.5°W) at 125m. From Levitus et al. (1994).

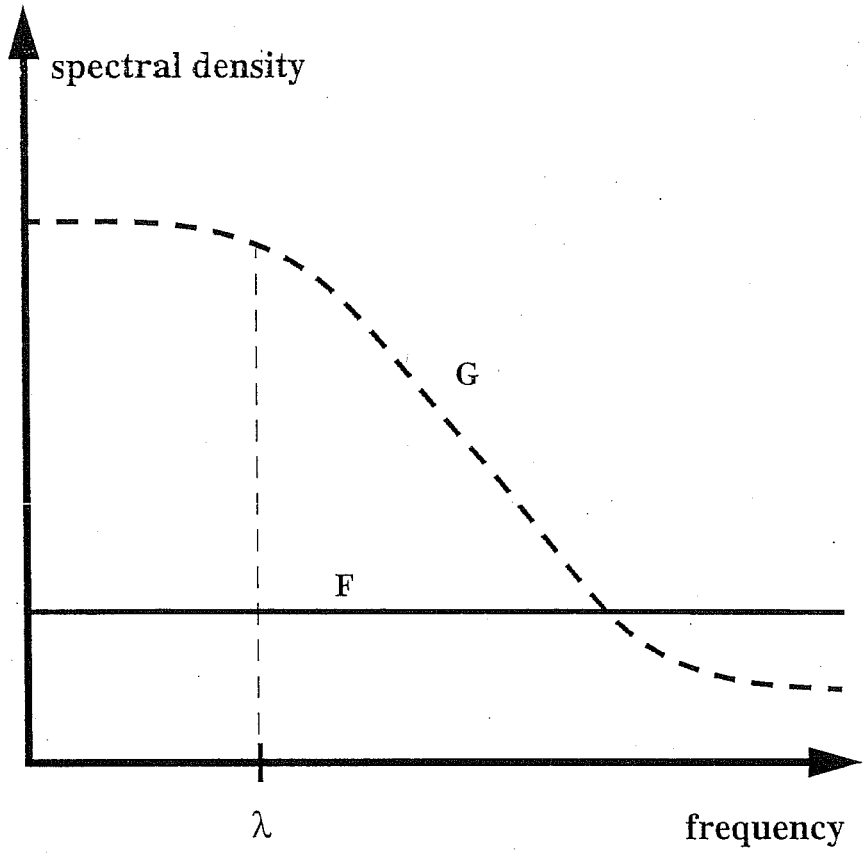


Fig. 5: Schematic input spectrum F and response spectrum G which result from the simplest version of the stochastic climate model (1). The atmospheric input spectrum is white, while the oceanic response spectrum is red down to a frequency which is determined by the damping λ.

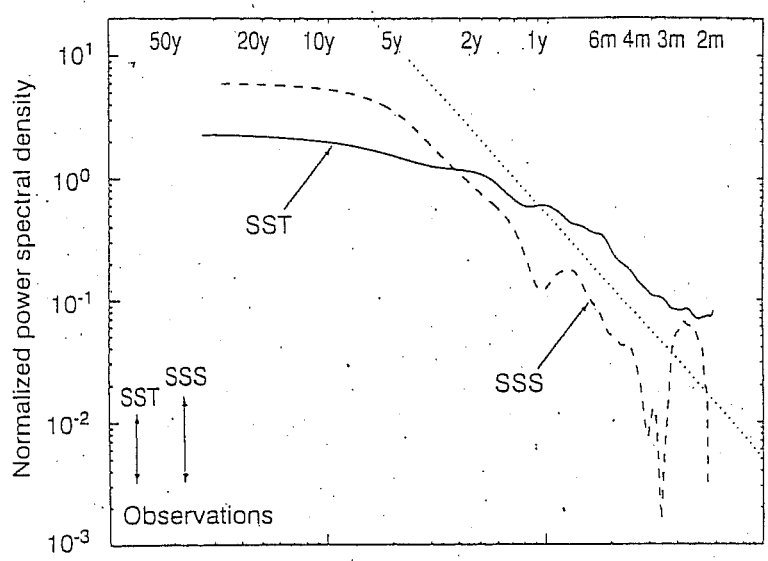


Fig. 6: Spectra of anomalous North Atlantic SST and SSS observed at ocean weather ship 'I' (60.8°N, 20.6°W). The dotted line shows the slope $\omega^{-2}$. From Hall and Manabe (1997).

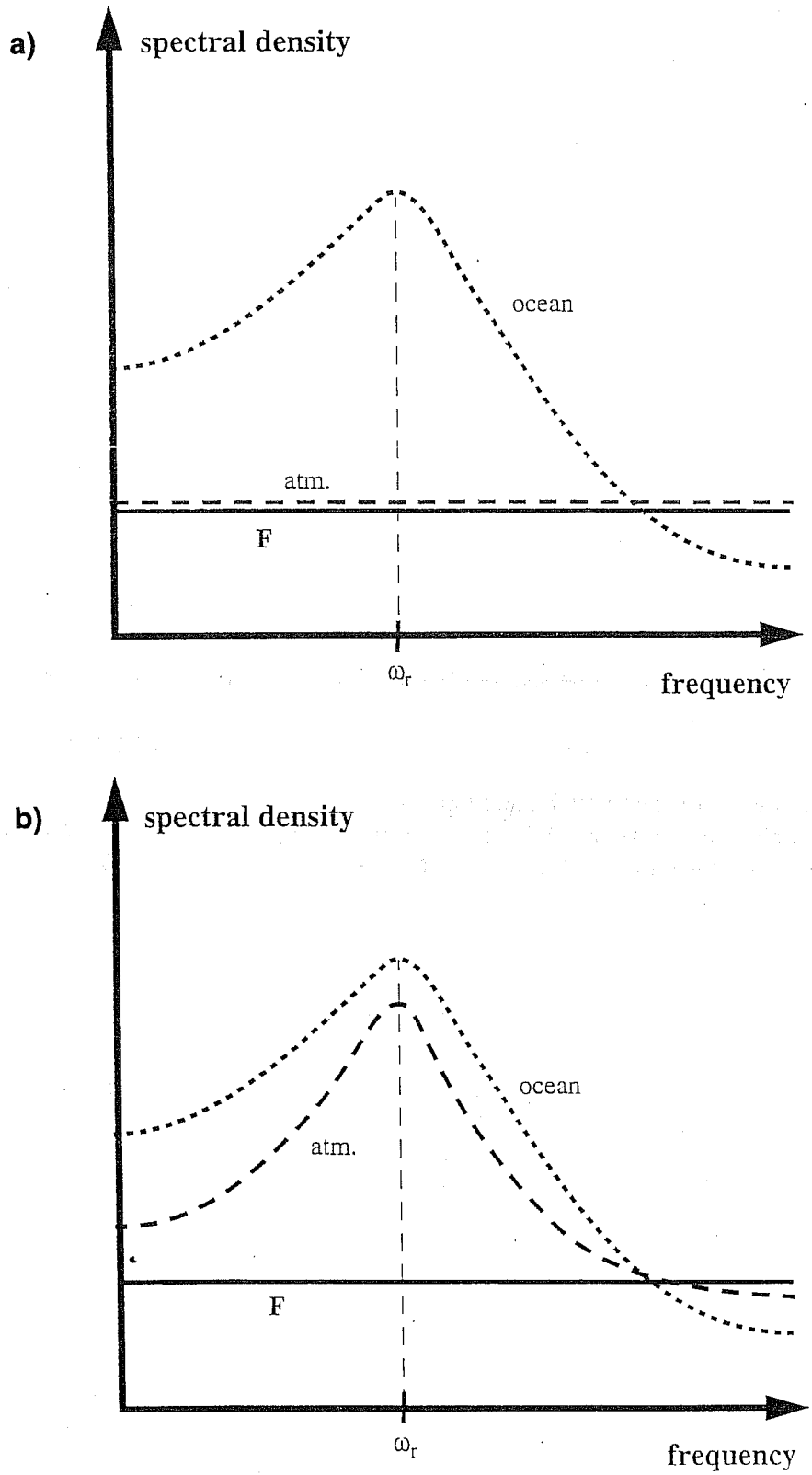


Fig. 7: Schematic atmospheric and oceanic spectra which result from the stochastic excitement of a) an 'ocean-only' mode and b) a 'coupled ocean-atmosphere' mode. In the former case, the atmospheric spectrum is white, while the oceanic spectrum shows a peak at the resonance frequency; in the latter case both the atmospheric and the oceanic spectra show a peak at the resonance frequency.

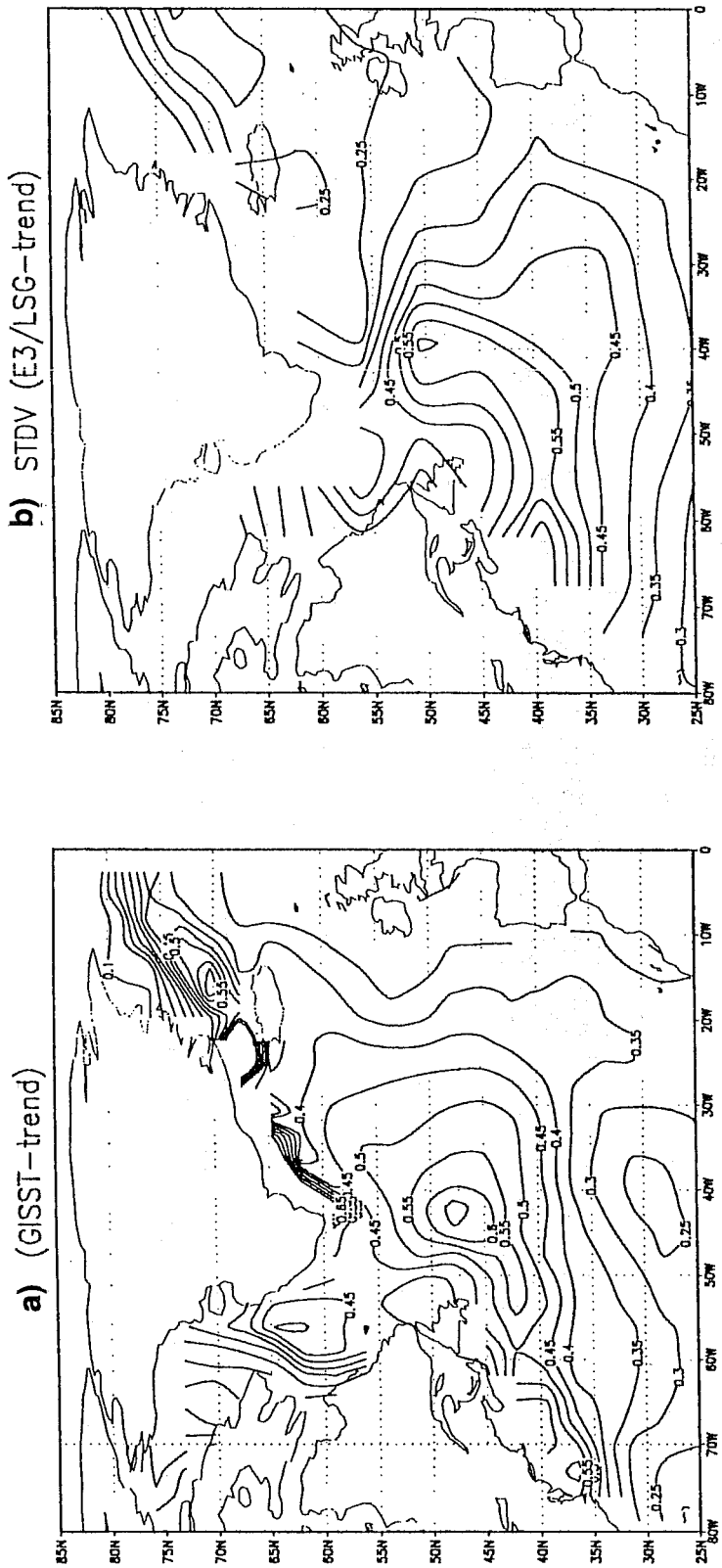


Fig. 8: Comparison of the SST standard deviations in the North Atlantic (computed using annually averaged values), as derived from a) the observations (GISST) and b) the coupled model simulation with the ECHAM3/LSG CGCM. From Timmermann et al. (1998).

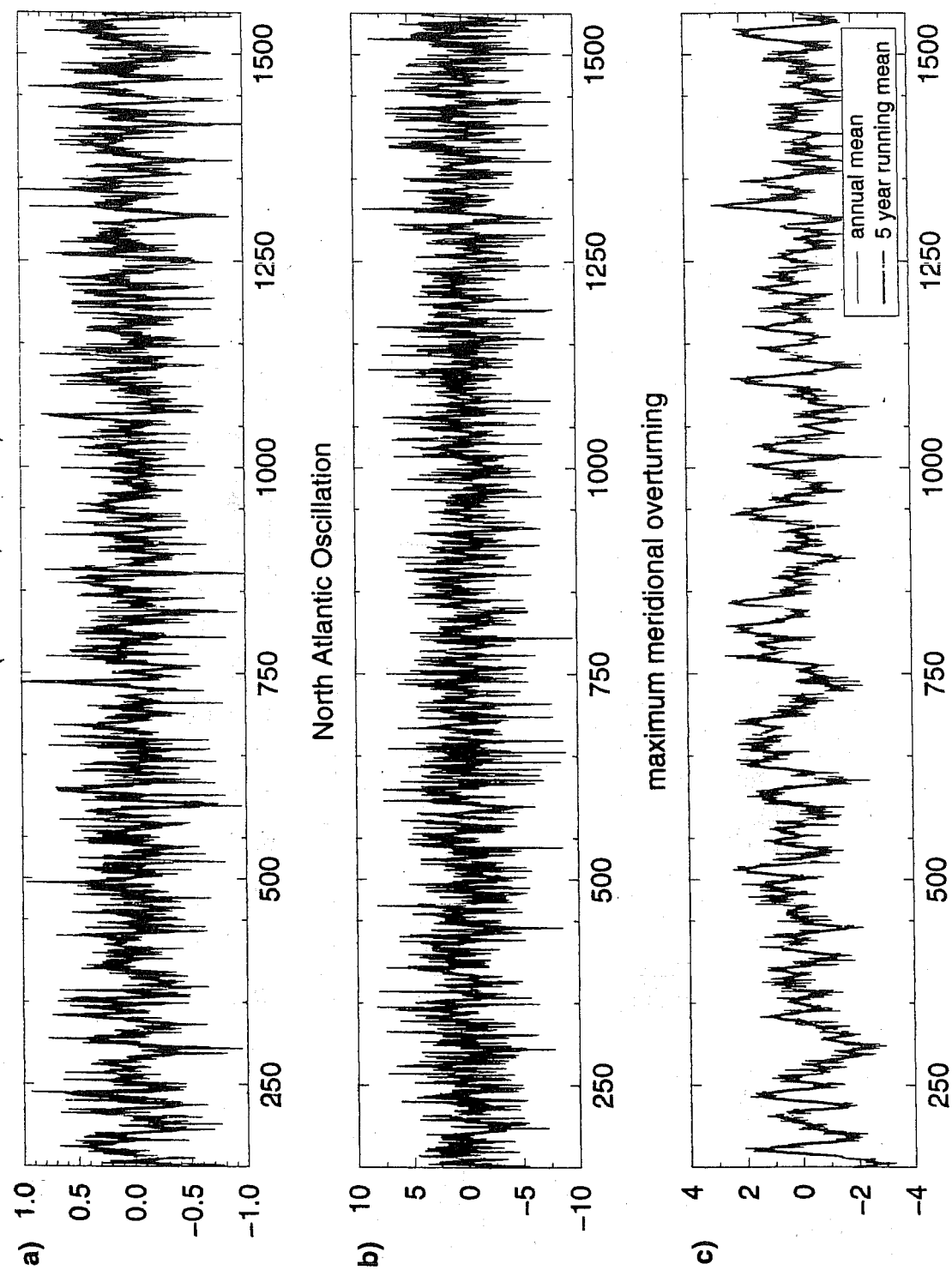


Fig. 9: Time series of anomalous North Atlantic a) SST (K), b) NAO, and c) meridional overturning (Sv) simulated by the the coupled model ECHAM3/LSG. From Grötzner (1999, pers. comm.).

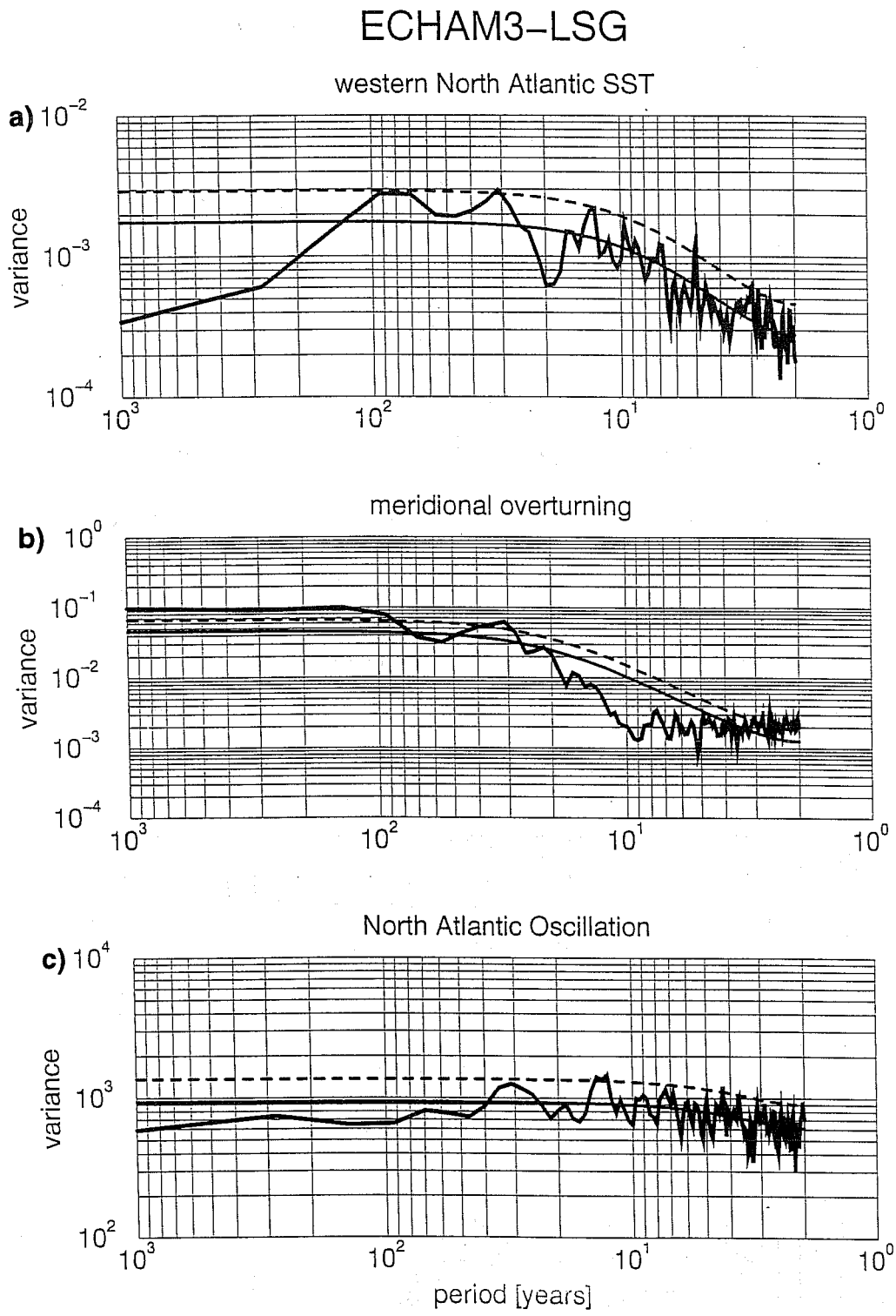


Fig. 10: Spectra of the anomalous North Atlantic a) SST, b) meridional overturning, and c) NAO shown in Fig. 9. From Grötzner et al (1999, pers. comm.).

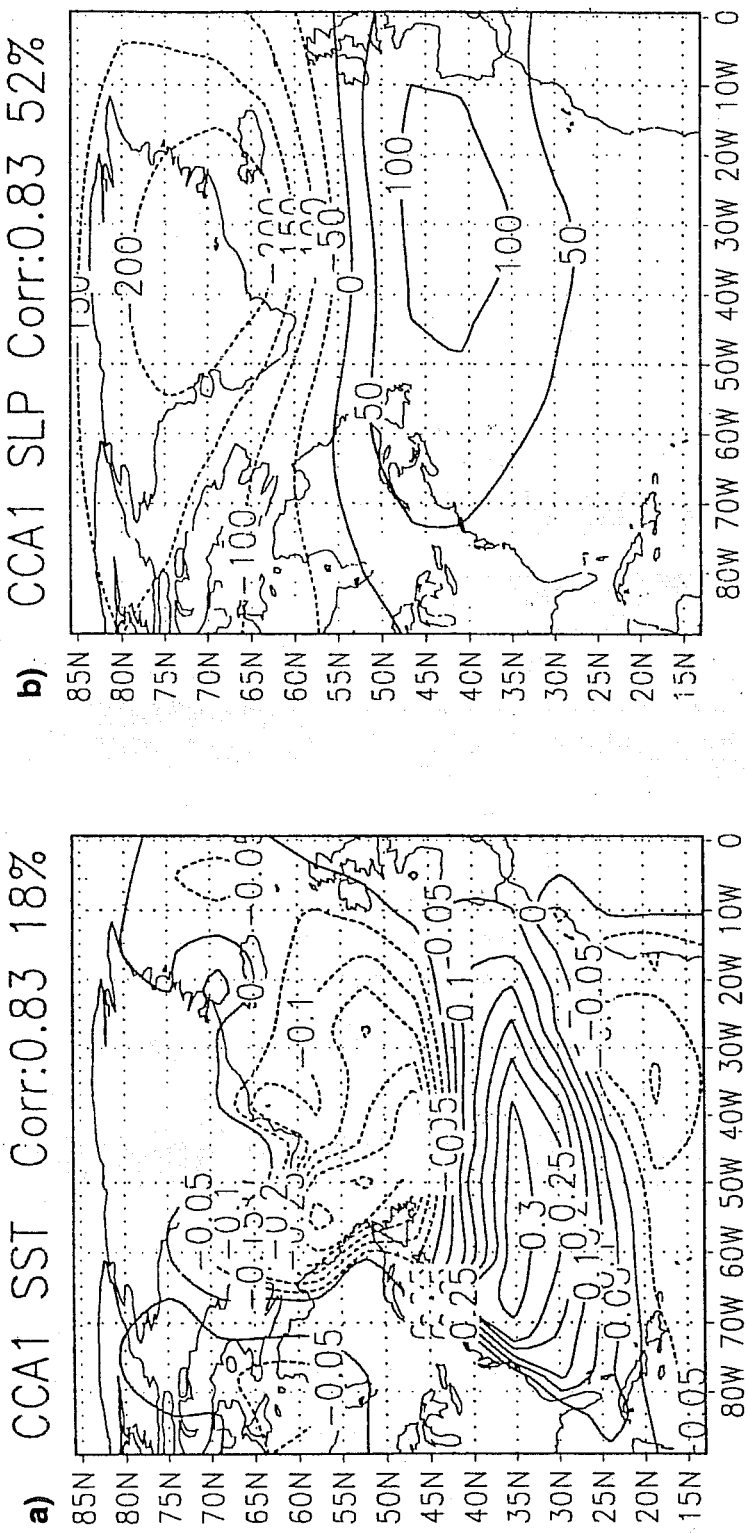


Fig. 11: a) North Atlantic SST anomaly and b) SLP anomaly fields as derived from the leading CCA mode. These patterns are characteristic of the quasi-decadal mode. From Timmermann (1996).

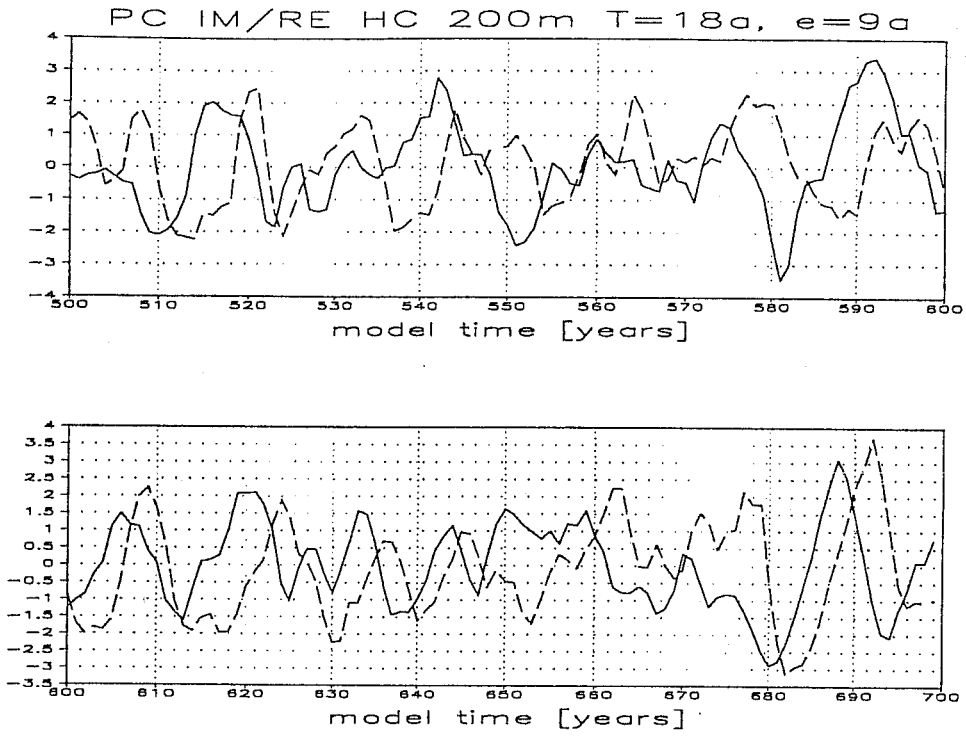


Fig. 12: Time series of the leading POP mode of North Atlantic upper ocean heat content (0-200m) anomalies. The POP analysis has been performed using the model years 500-700. The dashed line shows the real part and the solid line the imaginary part. The real part time series is highly coherent with those of the leading CCA mode (with opposite signs). From Timmermann (1996).

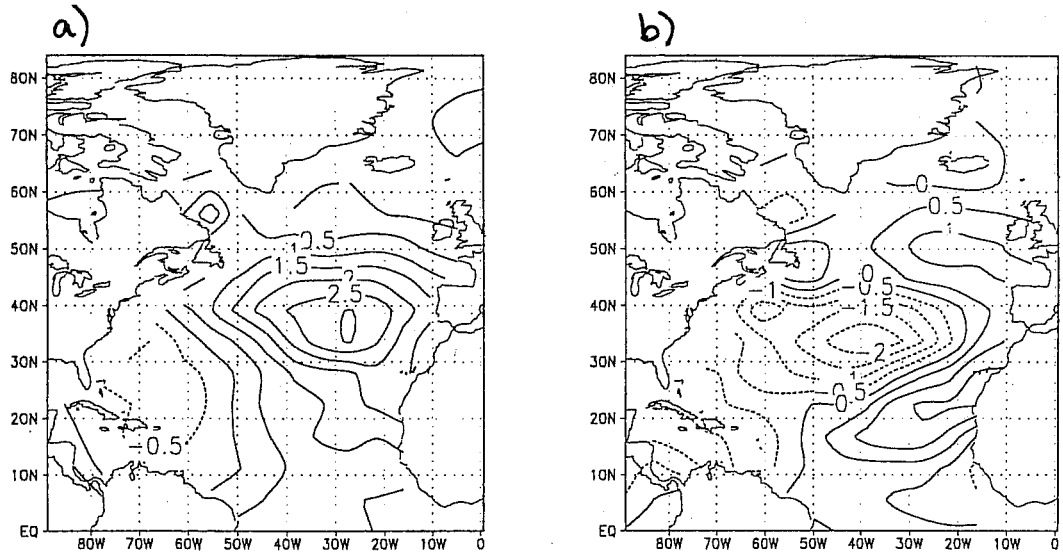


Fig. 13: a) Imaginary and b) real part patterns of the leading POP mode of upper ocean heat content anomalies. The two POP patterns describe a clockwise rotation of the heat content anomalies. From Timmermann (1996).

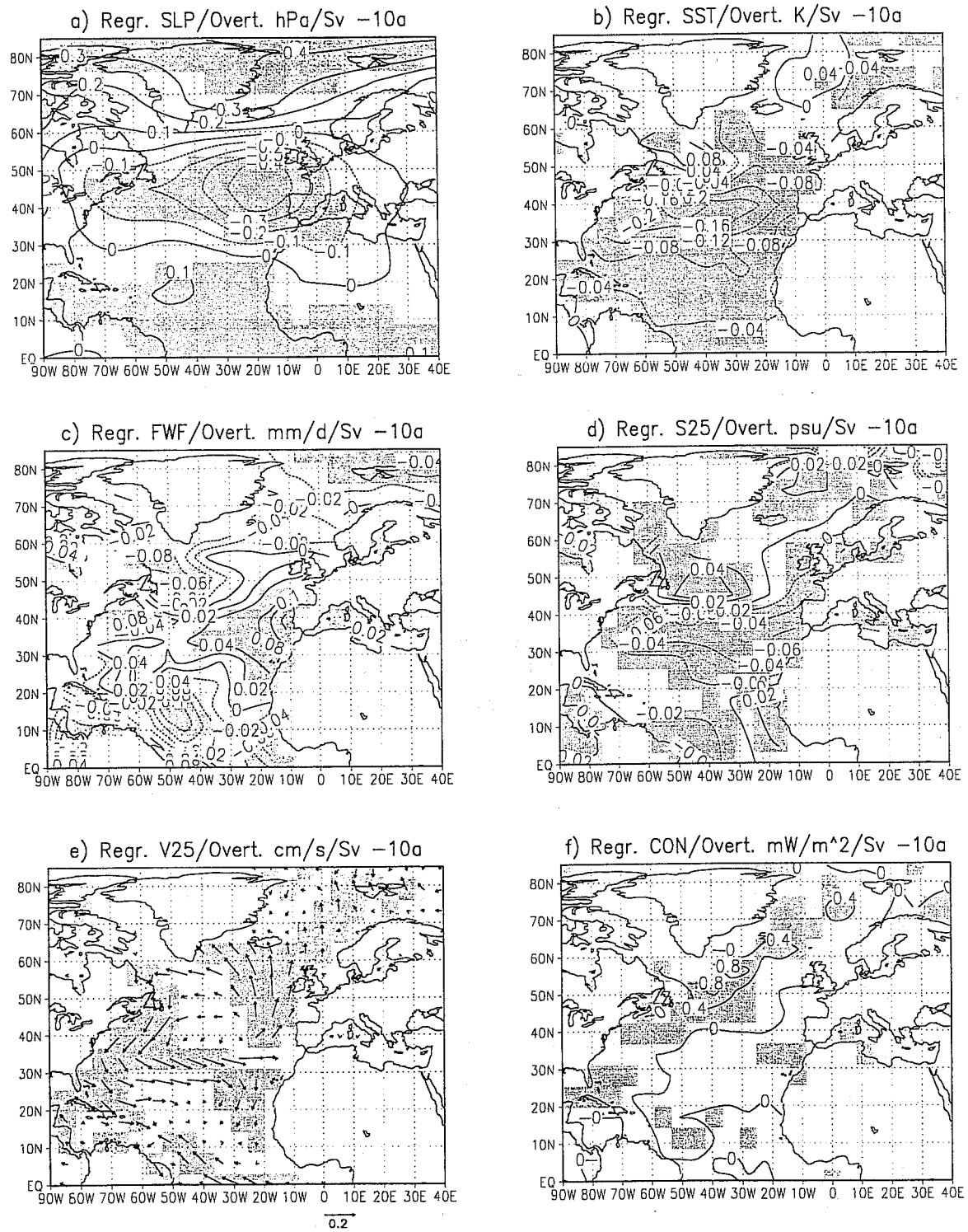


Fig. 14: Maps of lagged regression coefficients of selected anomaly fields (lag -10 years, i. e. the fields show the conditions 10 years prior to the maximum overturning). a) SLP (hPa/Sv), b) SST (K/Sv), c) fresh water flux (mm/d/Sv), d) SSS (psu/Sv), e) surface currents ((cm/s)/Sv), and f) loss of potential energy by convection [(mW/m$^2$)/Sv]. The shading denotes regions in which the results are statistically significant at the 95% level. From Timmermann et al. (1998).

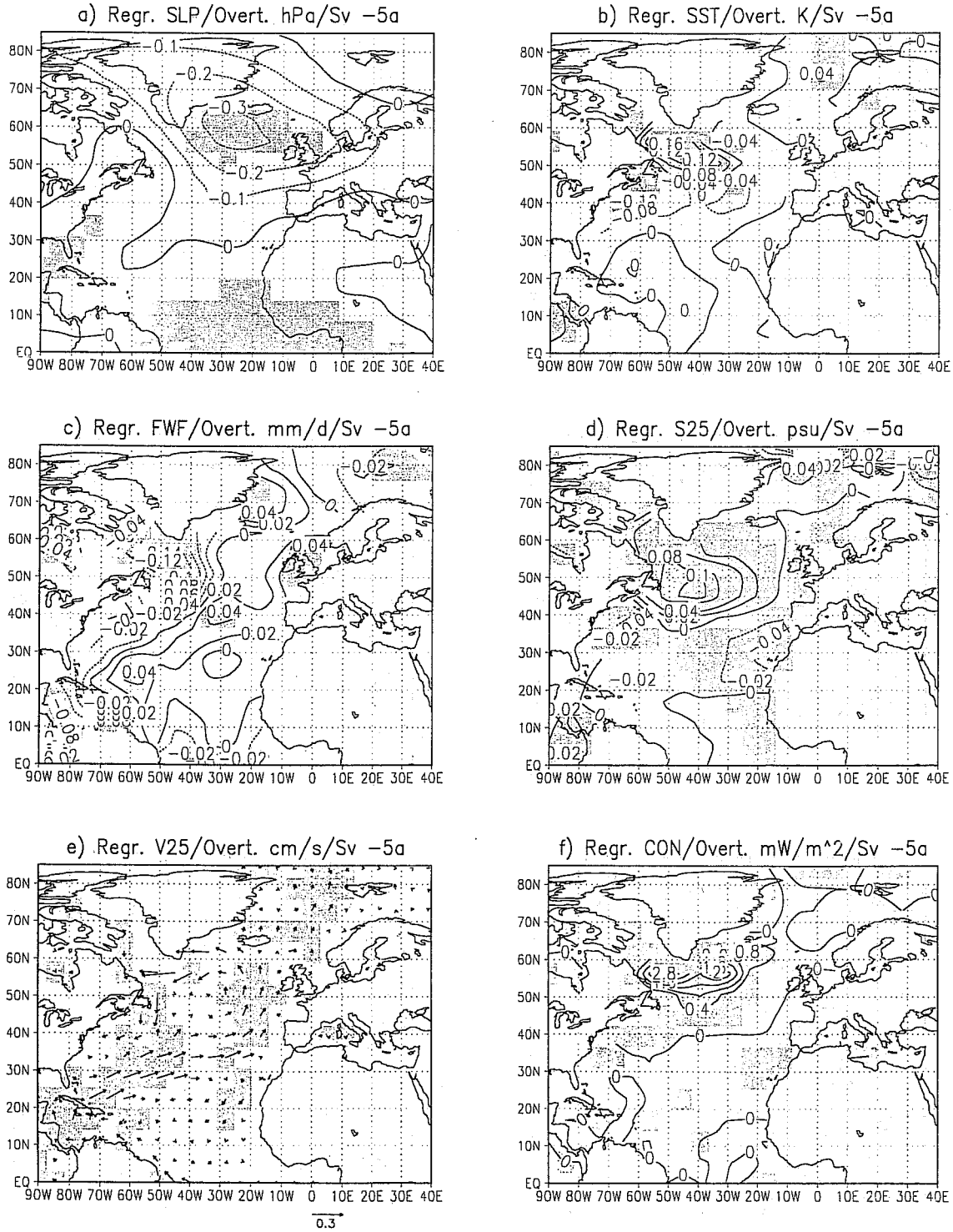


Fig. 15: Maps of lagged regression coefficients of selected anomaly fields (lag -5 years, i. e. the fields show the conditions 5 years prior to the maximum overturning). a) SLP (hPa/Sv), b) SST (K/Sv), c) fresh water flux (mm/d/Sv), d) SSS (psu/Sv), e) surface currents ((cm/s)/Sv), and f) loss of potential energy by convection [(mW/m$^2$)/Sv]. The shading denotes regions in which the results are statistically significant at the 95% level. From Timmermann et al. (1998).

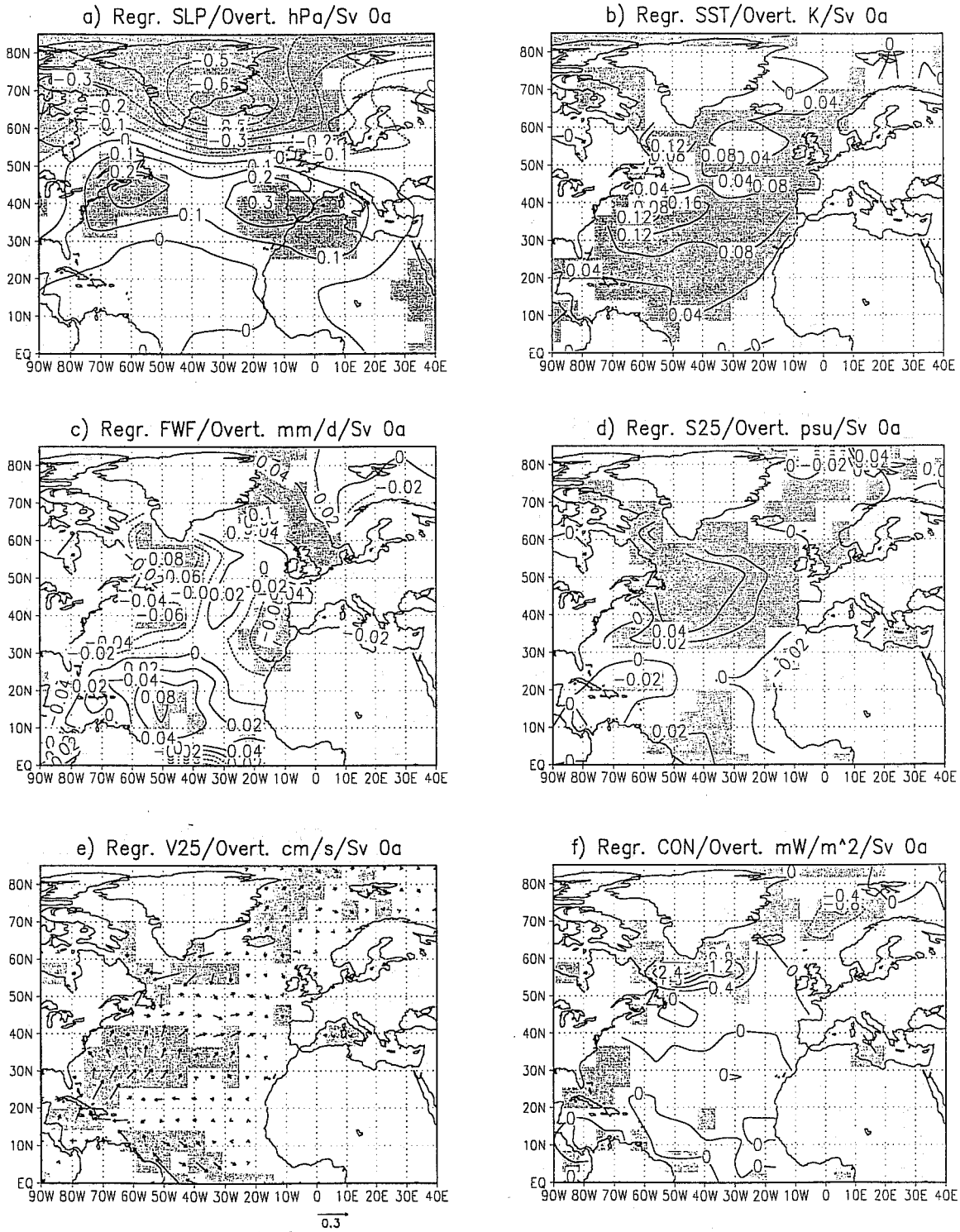


Fig. 16: Maps of lagged regression coefficients of selected anomaly fields (lag 0 years, i. e. the fields show the conditions at the time of the maximum overturning). a) SLP (hPa/Sv), b) SST (K/Sv), c) fresh water flux (mm/d/Sv), d) SSS (psu/Sv), e) surface currents ((cm/s)/Sv), and f) loss of potential energy by convection [(mW/m$^2$)/Sv]. The shading denotes regions in which the results are statistically significant at the 95% level. From Timmermann et al. (1998).

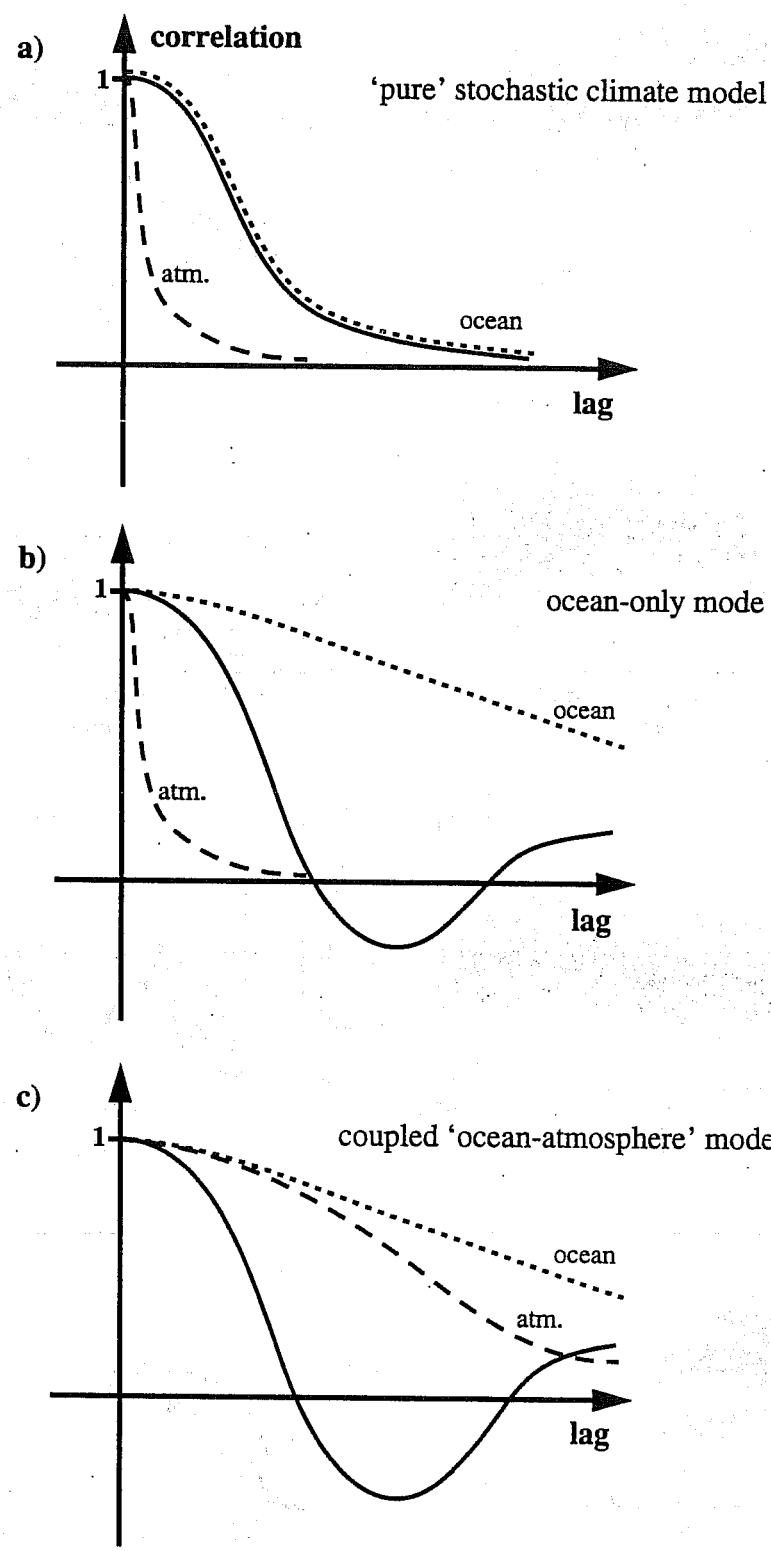


Fig. 17: Schematic atmospheric and oceanic skills expected from three scenarios. a) The 'pure' stochastic climate model, b) the stochastic excitement of an 'ocean-only', c) the stochastic excitement of a 'coupled ocean-atmosphere' mode. The persistence of a typical oceanic quantity (such as the anomalous SST) is given by the full lines. The typical oceanic skills are given by the dotted lines, while those of typical atmospheric quantitities are given by the dashed lines.

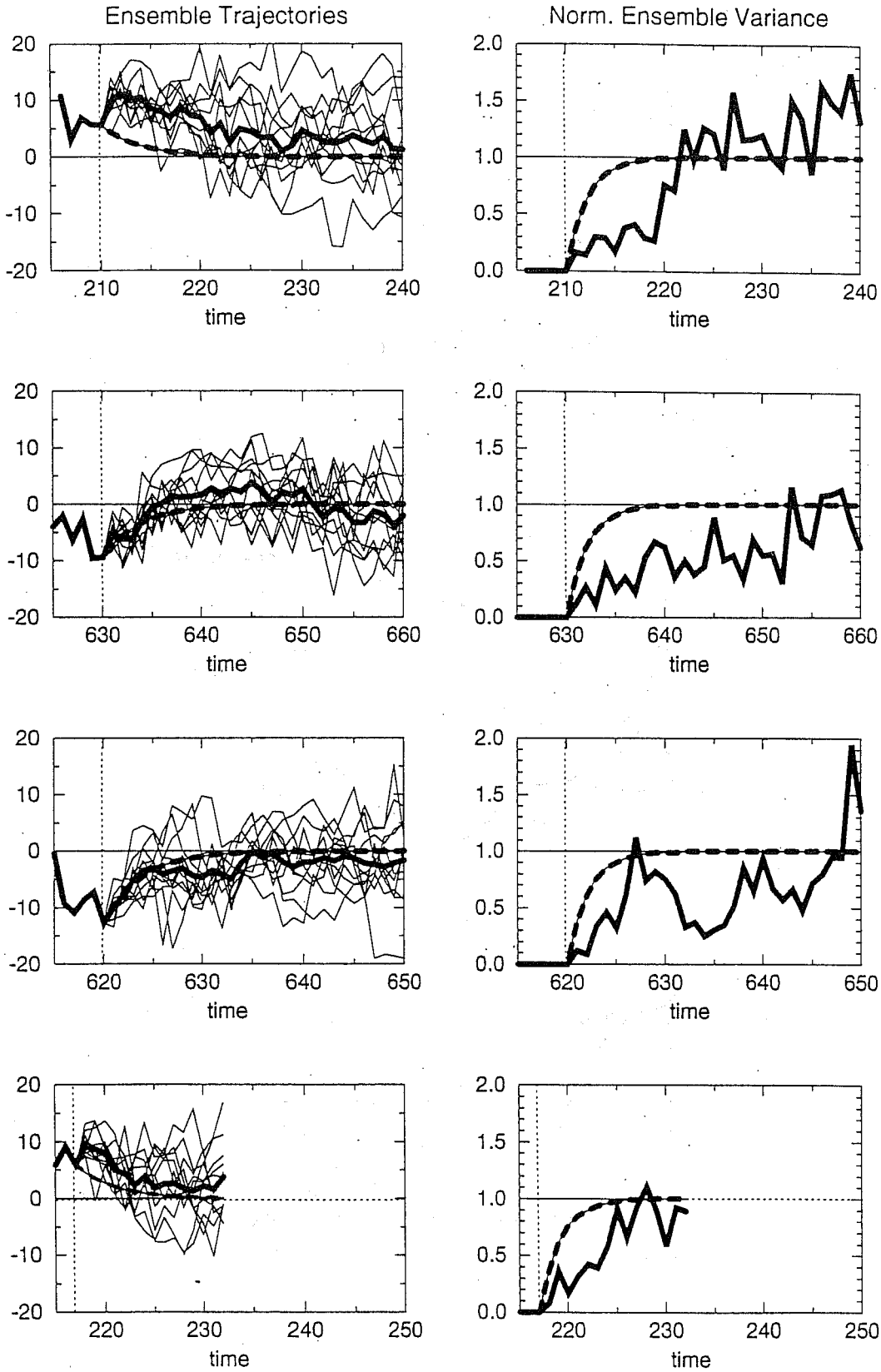


Fig. 18: Individual ensemble trajectories and ensemble mean (thick line) of projections onto the first EOF of the anomalous North Atlantic meridional overturning for the four different forecast ensembles (left) and time series of the respective normalised ensemble variances (right). The thick dashed lines show the temporal behavior of fitted first order autoregressive processes. From Grötzner et al. (1999).

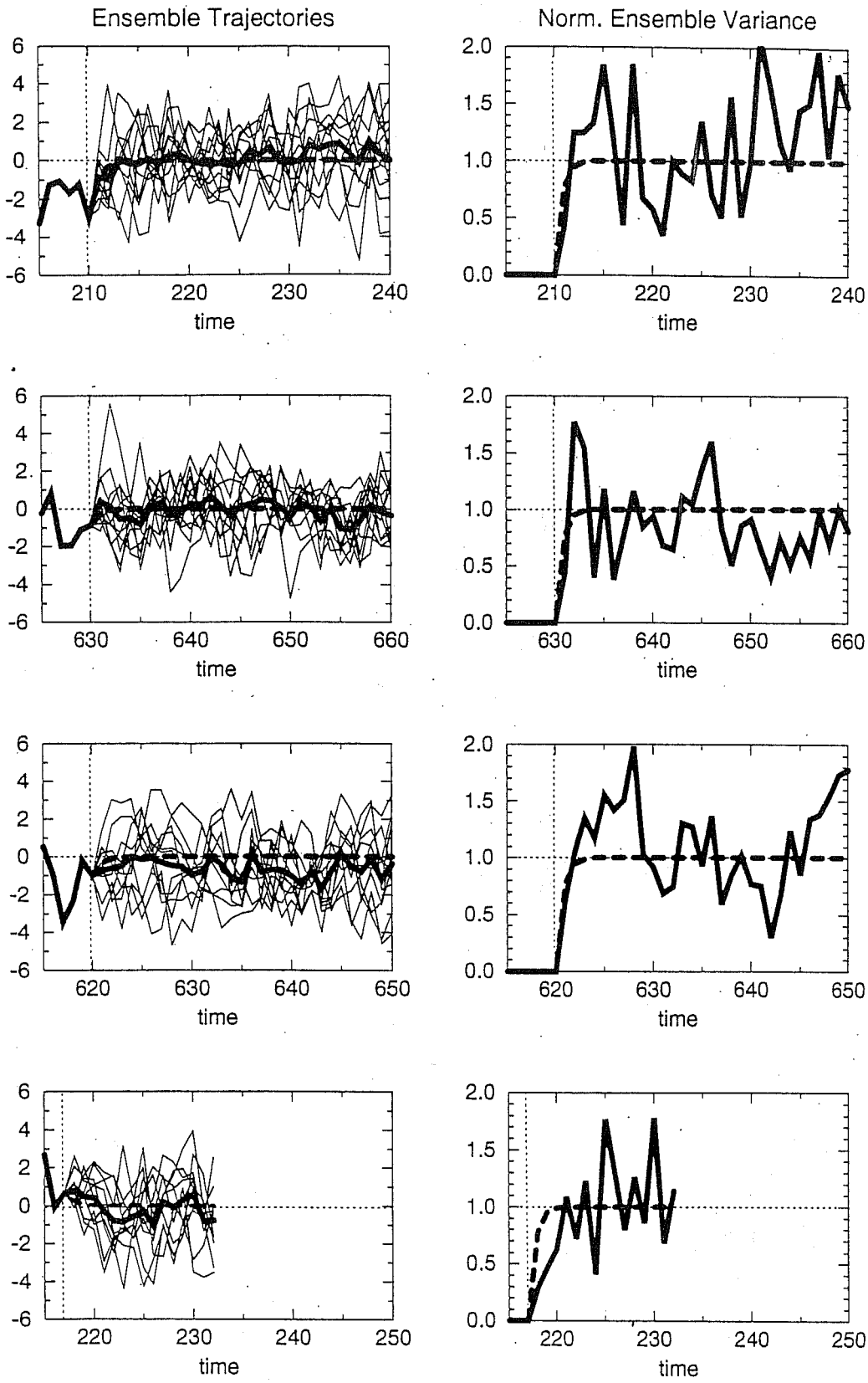


Fig. 19: Individual ensemble trajectories and ensemble mean (thick line) of projections onto the first EOF of the North Atlantic SST anomalies for the four different forecast ensembles (left) and time series of the respective normalised ensemble variances (right). The thick dashed lines show the temporal behavior of fitted first order autoregressive processes. From Grötzner et al. (1999).

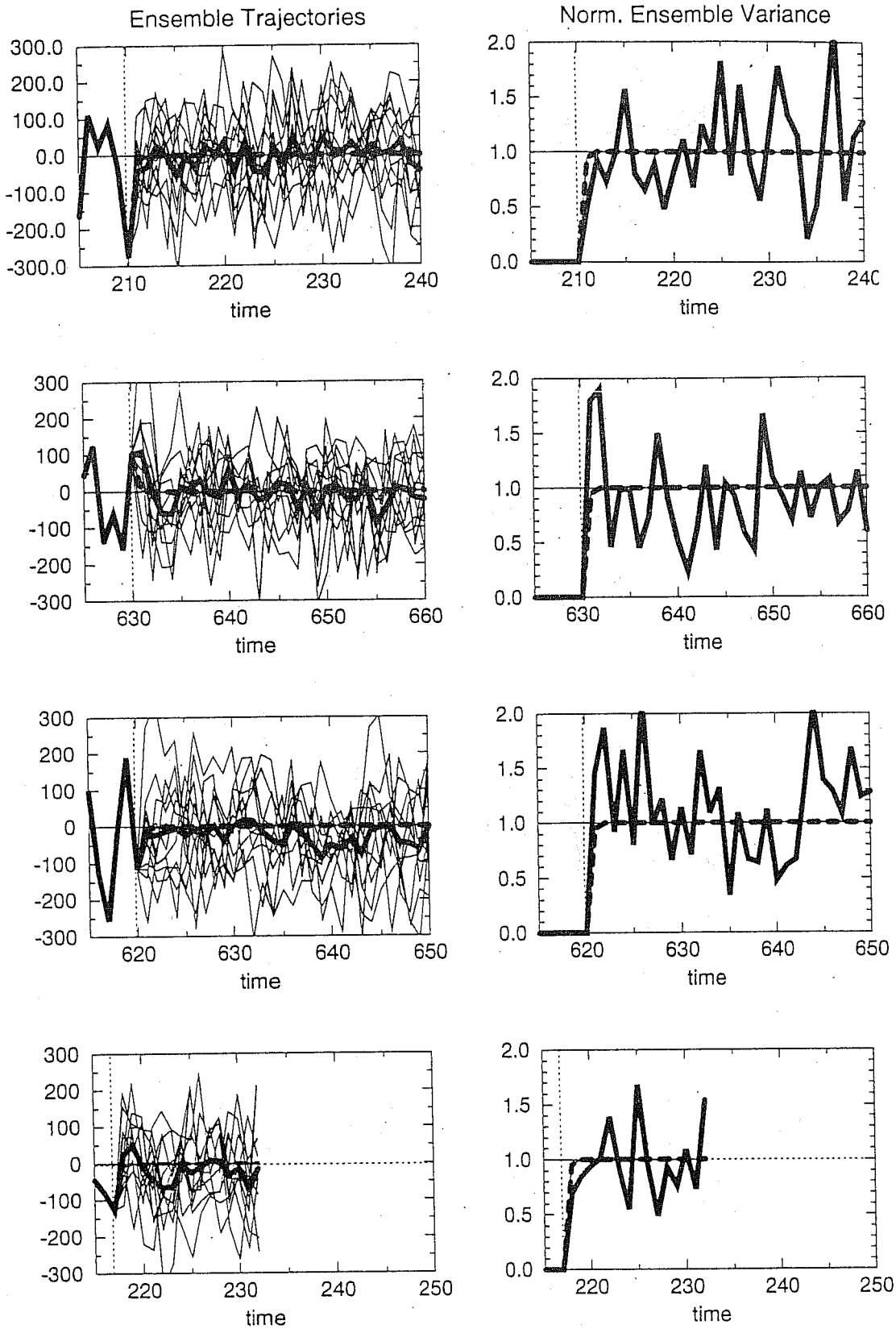


Fig. 20: Individual ensemble trajectories and ensemble mean (thick line) of projections onto the first EOF of the North Atlantic 500 hPa geopotential height anomalies for the four different forecast ensembles (left) and time series of the respective normalised ensemble variances (right). The thick dashed lines show the temporal behavior of fitted first order autoregressive processes. From Grötzner et al. (1999).